19th INTERNATIONAL CONGRESS ON ACOUSTICS
MADRID, 2-7 SEPTEMBER 2007

CAVITATION AND CETACEAN

PACS: 43.30.-k

Leighton, Timothy G.; Finfer, Daniel C.; White, Paul R.
Institute of Sound and Vibration Research, University of Southampton, Southampton S017 1BJ, United Kingdom; tgl@soton.ac.uk (http://www.isvr.soton.ac.uk/fdag/UAUA/Cetaceans.HTM)

ABSTRACT
Bubbles are the most acoustically active naturally occurring entities in the ocean, and cetaceans are the most intelligent. Having evolved over tens of millions of years to cope with the underwater acoustic environment, cetaceans may have developed techniques from which we could learn. This paper outlines some of the possible interactions, ranging from the exploitation of acoustics in bubble nets to trap prey, to techniques for echolocating in bubbly water, to the possibility that man-made sonar signals could be responsible for bubble generation and death within cetaceans.

INTRODUCTION
Acoustics affects our lives profoundly and commonly, both as a nuisance and a necessity. Through speech, acoustics has dominated our communications for millennia. It underpins not only recorded music but also live transmissions, from entertainment in theatres and concert venues to public address systems. Although our experience for millennia has been dominated by audiofrequency sound in air, today we use ultrasound in liquids for biomedical diagnosis and therapy, for sonochemistry and ultrasonic cleaning, and for the monitoring and preparation of foodstuffs, pharmaceuticals and other domestic products. From the Second World War to the present conflicts, acoustics has had an unrivalled role in the underwater battlespace. Underwater sound sources are used to map petrochemical reserves and archaeological sites, as well as to monitor a huge variety of important commercial and environmental features, from fish stocks to climate change.

Many of these applications in ocean acoustics, sonochemistry, biomedical ultrasonics etc. involve the passage of sound or ultrasound through liquid or liquid-like media. When sound at frequencies of ~1 kHz or greater is passed through water in the natural world, gas bubbles are the most potent naturally-occurring entities that influence the acoustic propagation, if they are present [1-4]. However our experience as humans of audiofrequency sound in air does not equip us with an intuitive appreciation of the acoustic environment in liquids. With 20 million years or so in which to evolve systems and solutions, the mammals with greatest experience of using acoustics in bubbly water are cetaceans (whales, dolphins and porpoises). Given the complexity and potency of gas bubbles in liquids, and the potential for their exploitation, this paper addresses the question of whether there is anything we can learn from the acoustical response of cetaceans to the bubbly marine environment [1, 5, 6].

The problem is particularly apt given that, whilst most of human sonar was developed for us in the deep-water environments which typified the requirements of the Second World War and the Cold War, since the fall of the Berlin Wall the emphasis for military sonar has been on shallower waters, the so-called littoral zone. The development of human underwater sonar throughout the 20th Century concentrated on acoustic problems relevant to the deep-water threats which characterized the Cold War. Now however the requirement to detect large, quiet nuclear submarines passing under the Arctic icecap has been replaced by the requirement to detect quieter submarines (diesel electric) and obstacles and mines in shallower waters, to mitigate threats to commercial or humanitarian shipping or landing craft, or to detect diver incursions and saboteurs in harbours etc. Sonar expertise needs to develop to cope with this more challenging

environment, which can for example hide mines that can be relatively inexpensive, threaten civilian shipping and personnel as well as military, and which can interfere with operations if their absence or locations cannot be confirmed. With these new challenges has however come an impetus to explore how the transformation of acoustic propagation by complex environments may be used as a diagnostic tool for characterising that environment, from our oceans [7-9] to off-world environments [1, 10-14].

Acoustic signals do not usually propagate well in bubbly water, and yet whales, dolphins and porpoises not only function effectively in shallow coastal waters, but also at times generate large bubble fields to assist with catching prey. This paper outlines the challenges faced by cetaceans in using acoustics in such environments, and proposes acoustical techniques which would work. The validities of such proposed acoustical solutions are explored through theory, simulation and experimentation. The scenarios in question relate to the circular and spiral bubble nets generated to trap prey by humpback whales, and solutions to difficulties associated with echolocation by dolphins and porpoises in bubbly water. Whether the solutions are exploited by cetaceans is uncertain, but their efficacy in test tanks and implications for man-made sonar are demonstrated.

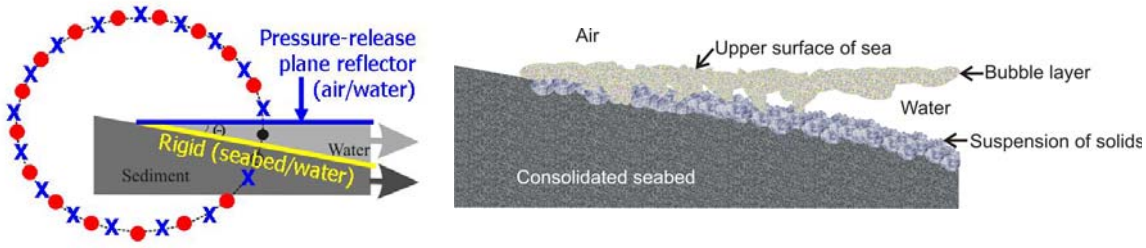

(a) (b)

Figure 1.- (a) If a coastal zone can be approximated by a wedge shape of ocean, with a bottom which reflects acoustic pressure waves with no phase change, and an air/water interface which reflects them with π phase change, then for frequencies high enough for a ray approach to be valid, the net sound field built up in the water by an object (●) emitting sound will be that which would be produced were the object in free-field, and sound were in addition emitted image sources either in phase (○) with the original source, or in antiphase (×). The sediment and atmosphere boundaries of the water column being flat acoustic mirrors in this model, in the 2D plane passing vertically through the source these images will be distributed around the circle shown by the dashed line. The first few image sources are shown (○,×). For certain wedge angles Θ (such as the 15º used here) the sources map onto discrete sites on the dashed circle. (b) In this more realistic diagrammatic representation of the coastal zone, both the sea-air interface and consolidated seabed are more complicated reflectors than in (a). The air/sea interface will not only undulate with the passing of surface waves, but be punctuated with the noisy entrainment of bubble clouds. These bubbles can persist for many minutes against buoyancy, forming a dynamic sub-surface bubble layer which will attenuate and scatter acoustic signals (potentially nonlinearly), and can alter the sound speed by +/-50% or more. Likewise, the near-bottom suspended solids will scatter and attenuate sound travelling near the sea-bed, and may contain trapped gas which has attached itself to the solid particulate grains.

Figure 1 illustrates a classical picture of a wedge-shaped beach, as modelled for acoustical propagation [15, 16]. Even the simplest models indicate surroundings which have great potential to confuse a detection system which relies on active acoustic sonar. In Fig. 2(a) only the two most simple (i.e. time-invariant) acoustic scatterers in the coastal water column are included: the sediment and the air/water interface (both modelled as plane static reflectors). Even here a single target turns into a multitude (with appropriate time/phase delays). The case when the observer is itself the source of sound is particularly fascinating. A sound source in a wedge-shaped coastal waters can 'perceive' image sources; were such a simple wedge ever to exist, one can, for example, imagine how a single cetacean might see this as a ring of 'siblings'.

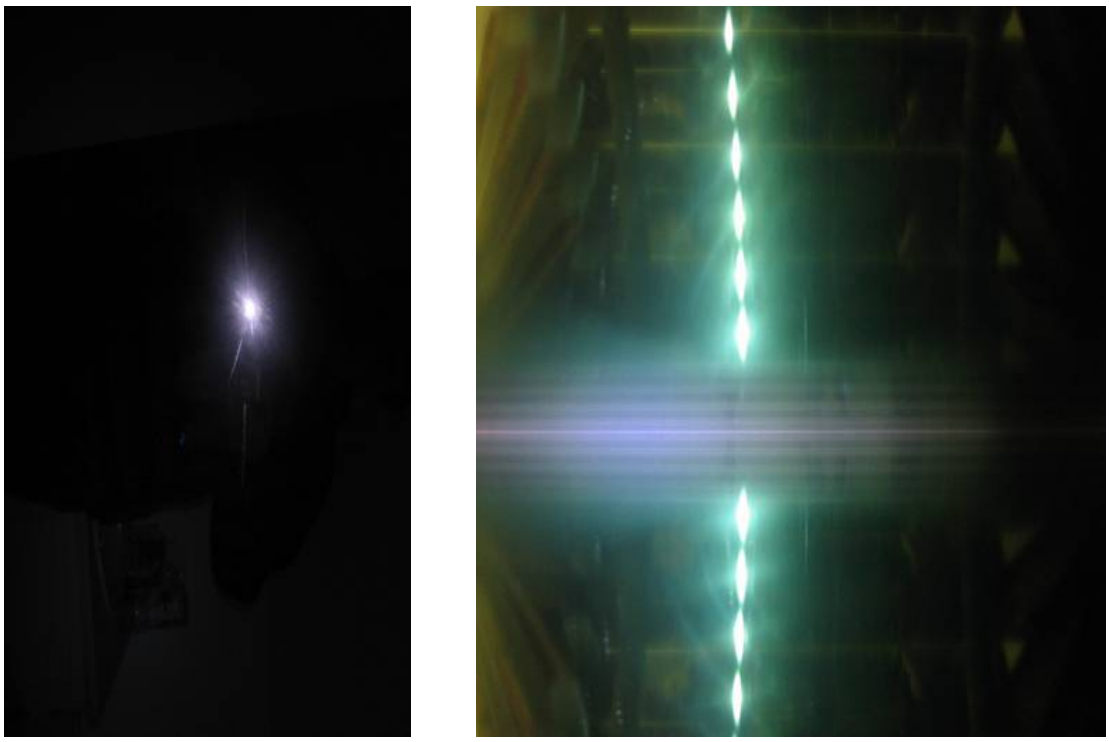

(a) (b)

Figure 2.- Image obtained by the observer when a torch (flashlight) is shone by the author (a) at a plane mirror and (b) into a 'wedge' formed by two angled planar mirrors.

Of course most coastal regions do not resemble the flat-sided wedge of Fig. 2(a). Real ocean coastlines provide features whose optical equivalents would be stranger than a carnival "hall of mirrors" [5], its floor covered by a fluctuating 'dry-ice fog' (the optical equivalent of suspended sediment particles), its wedge-shape complicated by ripples on the mirrored floor. Its ceiling would be an undulating, highly reflecting mirror, in some places focusing the sound in moving "hot spots" within the water column and floor, and in other places producing areas of dark, absorbing bubble clouds covered with a bright speckle of resonant bubble scatterers. Imagine those clouds being explosively generated by a breaking wave, then spreading over time. The optical equivalent of monostatic or bistatic sonar might involve one or more people with flashlights in this otherwise dark 'hall of mirrors'. The optical equivalent of nonlinearity would be if the flashlight emitted a strongly-attenuated red light in the carnival hall of mirrors; when, to compensate for this, the brightness of the flashlight is increased, blue new colours might be generated (the optical production of second-harmonic production, though of course the frequencies of blue light in the optical analogue is not twice that of red).

Therefore even if the sound speed were constant in time and the homogeneous throughout the ocean (as is the case for the speed of light in the visual equivalent of Figure 3), the shallow-water environment would be difficult enough to navigate in. However the presence of bubbles complicates matters significantly. Figure 4(a) shows the bubble size distribution measured at-sea. Whilst, if no bubbles were present, the sound speed would have been almost constant with frequency at ~1500 m s^{-1}, the addition of the bubble population of Figure 4(b) reduces the sound speed at low frequencies, leaves it relatively unaffected at high frequencies (in the absence if multiple scattering effects), and in the frequency range of 100 Hz to 100 kHz through-resonance effects are seen (Figure 4(b)). Figure 4(b) shows the extra attenuation which, it is calculated, the presence of this bubble population would impart. These behaviours can be readily understood from the slope of the maps of bubble volume against applied pressure, where the area mapped out corresponds to the dissipation and the slope corresponds to the sound speed [1, 3, 17]. Measured sound speed profiles and attenuations will be discussed in Figure 21). Hence bubble activity can reduce the sound speed dramatically (Birkin *et al.* [18] for example, measuring a sound speed reduction to nearly 50% of its original value in cavitating conditions).

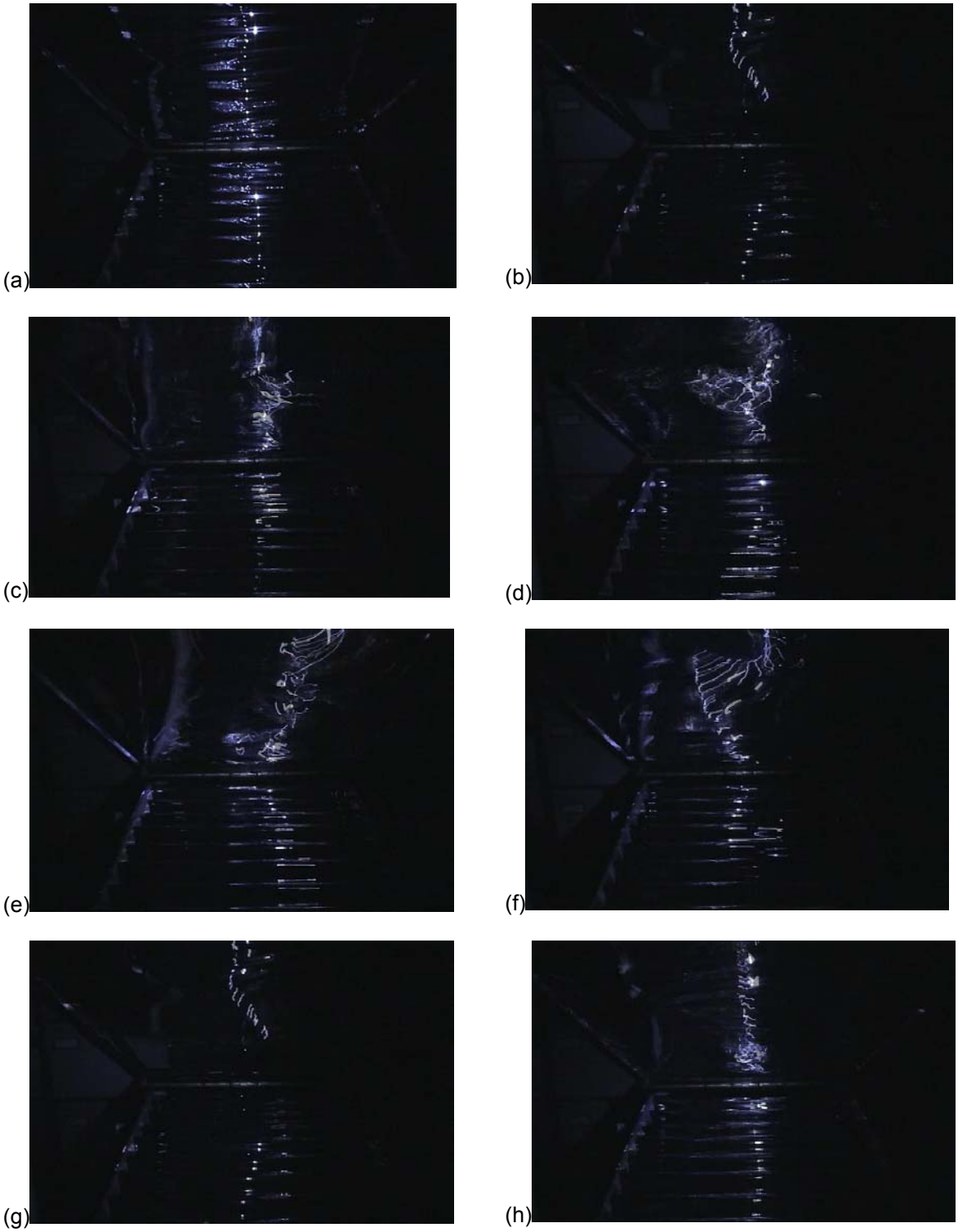

Figure 3.- The image obtained when the experiment of Figure 2(b) is repeated, but the bottom surface of the wedge is formed by plating a mirrored surface onto some corrugated plastic sheeting, and the top surface of the wedge has been made using a flexible mirror. In (a) the two surfaces are still; but for the images in parts (b) to (h), the upper surface is moved in a wave-like manner. To see a movie of this, go to http://www.isvr.soton.ac.uk/fdag/UAUA/Cetaceans.HTM

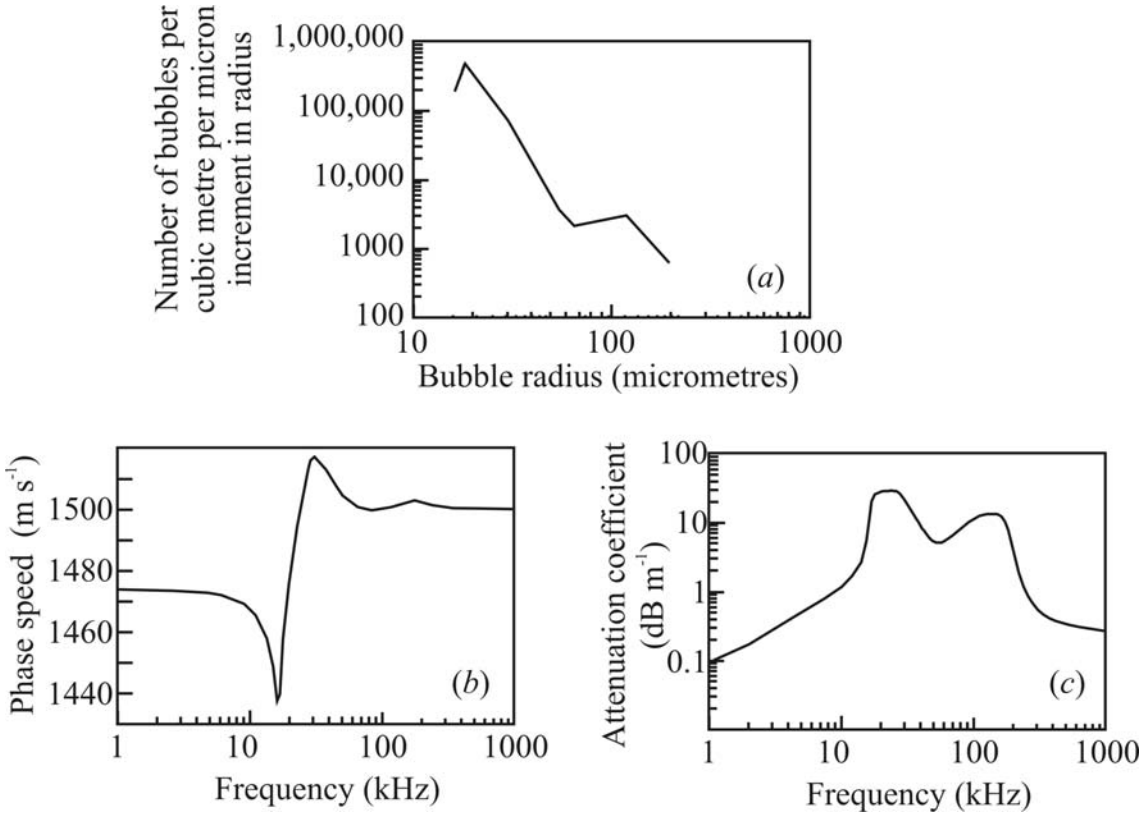

Figure 4.- (a) A bubble distribution function taken from a sea trial using the combination frequency technique. The mantissa plots the number of bubbles per cubic metre, per micron increment in radius. (b) Phase speed variations with frequency derived for the bubble population shown in (a). (c) The excess attenuation (i.e. that component of attenuation for which bubbles are responsible) with frequency derived for the bubble population shown in figure (a) (data from T. G. Leighton, S. D. Meers).

There are species of dolphin and porpoise (odontoceti) which inhabit shallow coastal waters. Consider the task faced by such creatures if they attempt to echolocate in such an environment. If a human were to find themselves suddenly in a world where the speed of light varied by factors of two on a sub-second timescale, they would no doubt find it almost impossible to function, and that is the circumstance in which the coastal odontoceti find themselves. However the key here is that the odontoceti have evolved in this environment. Given their intelligence, the possibility that odontoceti have found fascinating solutions to these acoustical challenging circumstances, and even that they are larger cetaceans could exploit these features, is a fascinating area for investigation. Given that the UK restricts measurements which can be made on cetaceans, a series of 'thought experiments' have been proposed by the author in which to explore this possibility [1, 5]. These will now be outlined in the following sections.

THE BUBBLE NETS OF HUMPBACK WHALES

This section will outline a hypothesis regarding one possible implication of the effects of bubbles on sound speed that were illustrated in Figure 4(c). Specifically, this is that low frequencies tend to experience a reduced sound speed in bubbly water. This led to a hypothesis [1, 5, 19] which might explain the mystery of the mechanism by which humpback whales (*Megaptera novaeangliae*) exploit bubble nets to catch fish.

It has been known for decades [20] that humpback whales, either singly or in groups, sometimes dive deep and then release bubbles to form the walls of a cylinder, the interior of which is relatively bubble-free (Figure 5(a,b)). The prey are trapped within this cylinder, for reasons previously unknown, before the whales 'lunge feed' on them from below (Figure 5(c)). In addition to the circular nets of Figure 5(b), spiral nets have also been photographed (Figure 6), although the relative frequency of circular, spiral, or other net geometries is not known [21]. Originally, an acoustical hypothesis for why the prey are trapped [1, 5, 19] was based on

circular bubble nets, because the bubble nets of humpback whales are frequently described as being 'circular' [20, 22-24]. This was followed by an acoustical hypothesis regarding spiral nets [12].

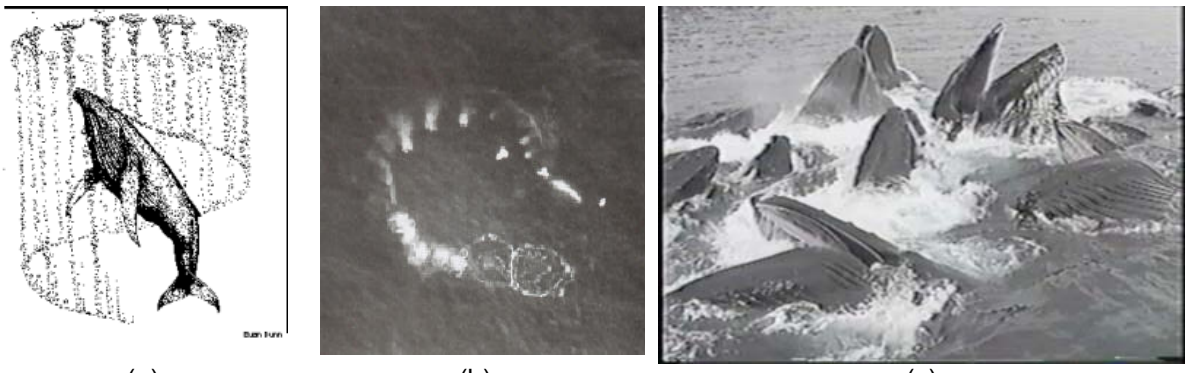

(a) (b) (c)

Figure 5.- (a) Schematic of a humpback whale creating a bubble net. A whale dives beneath a shoal of prey and slowly begins to spiral upwards, blowing bubbles as it does so, creating a hollow-cored cylindrical bubble net. The prey tend to congregate in the centre of the cylinder, which is relatively free of bubbles. Then the whale dives beneath the shoal, and swims up through the bubble-net with its mouth open to consume the prey ('lunge feeding'). Groups of whales may do this co-operatively (Image courtesy of Cetacea.org). (b) Aerial view of a humpback bubble net (photograph by A. Brayton, reproduced from reference [25]. The author has obtained permission from the publisher but has been unable to contact the photographer.) (c) Humpback whales lunge feeding (Image courtesy of L. Walker, http://www.groovedwhale.com).

Figure 6.- Three images illustrating the formation (a)-(c) of a spiral bubble net, with lunge-feeding occurring in frame (c). Note the presence of opportunistic birds. (Photographs by Tim Voorheis / www.gulfofmaineproductions.com. Photographs were taken in compliance with United States Federal regulations for aerial marine mammal observation).

It was proposed that humpback whales use bubble nets as acoustic waveguides to create a sonic trap for prey, as shown in Figure 7 [1, 5, 19]. When the whales form such nets, they emit very loud, 'trumpeting feeding calls' [26]. The available recordings containing energy up to at least 4 kHz. A suitable void fraction profile would cause the wall of the cylinder to act as a waveguide, creating a 'wall of sound' with a relatively quiet interior at the centre of the cylinder. Figure 7(a) illustrates schematically how the bubble nets may cause sound to be trapped within the bubbly region. This plan view shows a section of the bubble net, with the whale emitting sound from outside of it. As shown by the sound speed graph, the speed of sound varies across the bubbly region, with a minimum on the axis. As indicated in Figure 4(b), this will be the case for sound waves of frequencies which are less than the resonant frequencies of the individual bubbles, and where the bubble density is a maximum on the axis. The behaviour of the sound within the bubbly region can be described by Huygens' principle. The new position of a

propagating wavefront may be found from the envelope of the small Huygens wavelets spreading out from the previous position of the wavefront. Since the speed of sound near the centre line of the bubbly region is less than that nearer the edge, the wavelets near the axis will have smaller radii than those near the edge (since, in any finite small time, they travel less far). The wavefronts therefore change direction and refract towards the centreline of the region. Even if the interior is not bubble-free, similar refraction occurs in this model, provided the void fraction decreases as one moves into the cylinder interior.

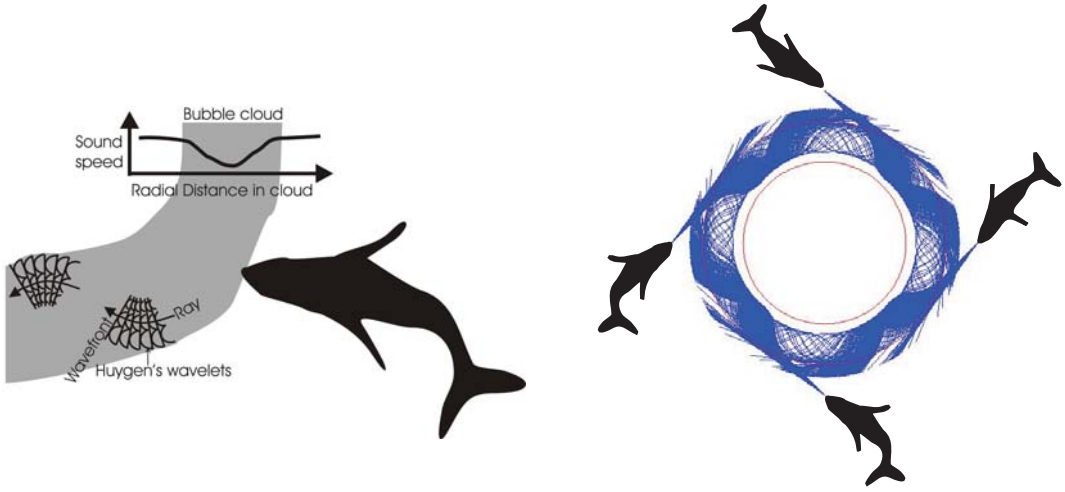

(a) (b)

Figure 7.- (a) Schematic of a whale insonifying a bubble-net (plan view), illustrating the sound speed profile in the cloud and, by Huygens' construction, sample ray paths. The sound speed profile assumes void fractions are greatest in the mid-line of the net wall, and assumes that the bubbles pulsate in stiffness mode. Hence the closer a Huygens wavelet is to the mid-line, the smaller the radius of the semicircle it forward-plots in a given time. Rays tend to refract towards the mid-line. (b) Plan view of four whales insonifying an annular bubble net (having 20 m mean diameter and a wall width of 4 m). Here the bubbles are driven in stiffness-controlled mode such that the sound speed decreases linearly from 1500 m/s at the walls (i.e. the sound speed in bubble-free water), to 750 m/s at the cloud midline (corresponding to a void fraction there of ~ 0.01%). The rays are coloured blue, and the locations of the inner and outer walls of the net are shown in red. Computed ray paths, where each whale launches 281 rays with an angular extent of 10°, refract as in (a). The rays gradually leak out, although some rays can propagate around the entire circumference. Plotting of a raypath is terminated when it is in isovelocity water and on a straight-line course which will not intersect the cloud. This refers to rays whose launch angles are such that they never intersect the net; and to rays which, having entered the net and undertaken two or more traverses of the mid-line, leave it [19]. For further details see http://www.isvr.soton.ac.uk/fdag/spiral_nets.htm

Figure 7(b) shows a two-dimensional ray diagram representing in plan view the interaction of sound with a bubble net. The bubble net is modelled as an annular region containing the bubble population, whilst the regions in the centre of and outside the annulus are free of bubbles. It is assumed that, just as for the oceanic bubble size distribution of Figure 4(b), the size distribution in the net is such that the sound speed in the walls of the net will be lower than that in bubble-free water for the <4 kHz insonification used by the whales.

The hypothesis is that any prey which attempted to leave the trap prey would enter a region where the sound is subjectively loud, be startled, and in response school (the bubble net turning the 'schooling' survival response into an anti-survival response). Furthermore, the trumpeting calls encountered in the 'wall of sound' were appropriate for exciting swim bladder resonances in the prey [1, 5, 12, 27, 28]. Either or both effects could encourage the prey to remain within the bubble net, and so trap them ready for consumption. The natural schooling response of fish to

startling would, in the bubble net, be transformed from a survival response into one that aids the predator in feeding.

There are however inefficiencies associated with the circular bubble net. To generate a 'wall of sound' of the form shown in Figure 7(b), the insonification needs to be tangential to the walls and, even if it is, the waves which propagate within the bubbly layer are attenuated and scattered by the bubbles (Figure 4(c)). Whilst of course sufficient attenuation on its own could generate a 'wall of sound' by simply preventing sound levels within the bubble net from attaining significant values, the refractive component of the 'wall of sound' required both tangential insonification and, if the attenuation were sufficiently great, the sound field might need reinforcing by other whales to generate a complete wall (as in Figure 7(b)). Furthermore, rays which refract out of the net are effectively wasted energy as they cannot be recaptured by the 'wall of sound'.

The spiral bubble nets of Figure 6 do not suffer from these disadvantages [12, 21]. Just a in the circular bubble net of Figure 7(b), the propagating rays which form the 'wall of sound' can be confined within bubbly water by refraction. However in both cases the rays trapped by refraction propagate through bubbly water, where the attenuation is greater than it would be for bubble-free water. It is therefore advantageous in forming a 'wall of sound' that the spiral bubble nets contain a second, complementary path, where the containment of the rays works through reflection, and crucially, the propagation occurs through bubble-free water where the attenuation is less. Furthermore the open end of the spiral forms a more robust entry point for the sound, and does not require shallow angles of the sort shown in Figure 7(b) in order to create a wall of sound with a quiet interior. The trap is therefore much more tolerant to the positioning of the whale.

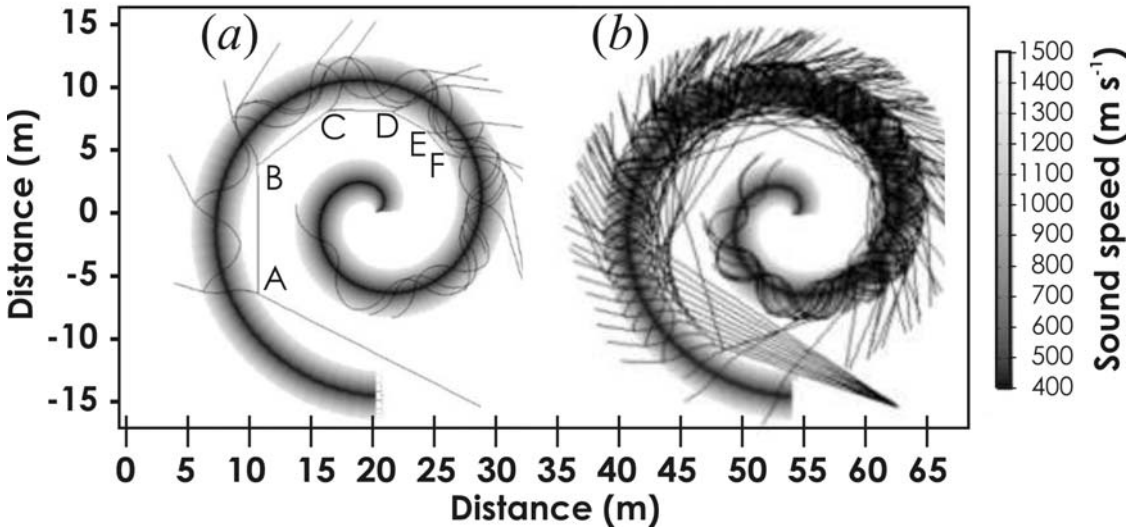

Figure 8.- Plan view of 2D spiral bubble net. (a) A single ray is launched. It reflects off the outer wall of the bubble-free arm of the spiral, the grazing angle decreasing each time (34º at A; 29 º at B; 23º at C; 19º at D; 16º at E; 13º at F). At each reflection, not only does a reflected ray propagate further into the bubble-free arm, but a refracted ray propagates into the bubbly-arm of the spiral. Attenuation is not included. (b) A beam of rays is launched into the spiral. The spiral generates clear regions which are both bubble-free and quiet (for further details see references [12, 21] and http://www.isvr.soton.ac.uk/fdag/spiral_nets.htm).

Consider just one ray as it enters the bubble-free arm of the spiral, as shown in Figure 8(a) (all modelling in this paper is restricted by the limitations of ray representation, as discussed earlier [19]). When it first meets the outer edge of the bubble-free arm (at the point labelled A, here with a grazing angle of 34º), the subsequent propagation is represented by two rays: a refracted ray in the bubbly arm, and a ray which is reflected into the bubble-free arm. The refracted ray propagates in the bubbly waveguide. As it approaches the edge of the bubbly water in principle it may of course be internally refracted back into the bubbly water. Alternatively a given ray may

intersect the edge of the bubbly waveguide, which in the model results in two rays propagating onwards: one is reflected back into the waveguide, whilst another is refracted into the bubble-free water (either within the spiral, or outside of it). Propagation within the bubbly waveguide is attenuated much more than propagation in the bubble-free arm. Because of the absence of attenuation in Figure 8(a), and because of the ability for rays to multiply at interfaces, there is of course no information in the figure with respect to acoustic intensity.

The ray which at A reflected into the bubble-free arm of the spiral, propagates through it until it next meets the bubbly water at B, with a reduced grazing angle (here, 29º). Again two rays are shown propagating away from B, a refracted ray (which recharges the attenuated sound field in the bubbly water), and a reflected ray which continues through the bubble-free water towards C. Further reflections at C, D etc. occur with reduced grazing angle, each one recharging the field in the bubbly water. The number of reflections is artificially truncated in the calculation at F.

The ever-reducing grazing angle will keep the inner edge of the bubbly net quiet, and the attenuation in the bubble cloud, and loss of energy from the ray in the bubble-free water each time it reflects, serve to reduce the sound field towards the centre of the spiral. In this way, quiet regions are generated. These are not just at the centre of the net, as with the circular net, but also along the inner edge of the bubble-free arm. Fish here will be in bubble-free, quiet water, but trapped within the spiral 'maze': in 2D, few positions will have an exit visible along the line of sight, and in real 3D nets the locations of the predators must be taken into account. Whilst Figure 8(a) showed the results (without attenuation) of the launching of a single ray into the spiral, Figure 8(b) shows a ray plot for the launching of a beam. As before, the plot lacks attenuation and requires the generation of both a refracted ray and a reflected one at interfaces, such that intensity information is incomplete. Note that the only rays with large grazing angles in the bubble-free arm have first propagated through the bubbly layer and suffered losses when refracting through the interface at least twice, and hence will be heavily attenuated.

There are clearly simplifications in Figure 8, some of which were discussed in reference [19]. As stated earlier, available recordings of the humpback call emitted during bubble net feeding contain significant energy in the 4 kHz range. The ray tracing approach used in the model presented here is appropriate for this frequency range, given the overall dimensions of the net. However, to understand the role of low frequency energy emitted during bubble net feeding, modal analysis would be required.

Figure 8 is, of course, two-dimensional representations, but the key elements would also pertain to a 3D spiral net. Therefore, should the whale emit its feeding call into the net from below, the propagation path in 3D can readily be visualised from this 2D representation. The walls of the net in Figures 8 are smooth and generate specular reflection, whilst the degree to which the walls of Figure 3 are rough is difficult to estimate, particularly as the visible shape of the net is dominated by the large bubbles: in contrast, the small bubbles can be less easy to see, but very potent acoustically. The roughness as perceived by the scattered acoustic field depends on the wavelength (λ) and the grazing angle (θ), such that the Rayleigh roughness criterion states a surface is rough if $kh\sin\theta = (2\pi/\lambda)h\sin\theta >> 1$, where h is the mean height of the surface undulations, and k is the wavenumber. In the absence of data on the geometry of the net which includes all bubbles[2], it is difficult to make calculations regarding smoothness. Because of the way the spiral continually reduces the grazing angle of rays as they penetrate further within it, then all else being equal, the inner regions of the spiral may therefore appear smoother, so creating robust regions within the spiral that are bubble-free and quiet. However this trend will be tempered by any change in h along the length of the spiral (reflecting the size of bubbles blown and the age of that portion of the net). The surface will appear most rough for the highest frequencies, which we take as 4 kHz [19]. For acoustic fields in bubble-free water, this gives a wavelength of 0.375 m, so that for test values of *h* of 0.1 m and 1 m, the wall will appear smooth for grazing angles less than about 37º and 4º respectively, with commensurately larger angles for lower frequencies. The angles compare well with the sequence of angles recorded in the caption to Figure 8(a).

Why some nets should be spiral is not clear. It may be a pragmatic or incidental response to practical limitations. Conceivably however the whales could be exploiting the different acoustical

properties of circular and spiral nets. These could confer possible advantages to the spiral configuration through the following features:

- A wall of sound can be generated using acoustic paths which propagate in bubble-free water (Figure 8) and hence suffer less attenuation than seen for acoustic paths in bubbly water (to which circular nets are restricted).

- Whilst both the bubble-free and bubbly paths in the spiral individually contribute to the wall of sound, the interactions between them create a synergistic effect: there will be ray paths which propagate at times in the bubble layer, and then leave it to enter the bubble-free layer, of the spiral; and reflections at interfaces between bubbly- and bubble-free water will be only partial. This has two advantages. First, whilst a ray which leaves the circular net is lost from the net, a ray which refracts out of a region of bubbly water in the spiral net can remain trapped within the spiral system. Specifically, when a ray leaves the circular bubble net of Figure 7(b) it is lost to the 'wall of sound'; but except for rays crossing the outermost interface of the spiral bubble net, rays crossing boundaries in the spiral net remain contained within it. Second, the field which propagates in the bubble-free arm of the spiral, can 'recharge' through refraction the more attenuated field within the bubbly arms (as occurs at the lettered points (A) to (F) in Figure 8(a)). This has the further advantage of attenuating the sound in the bubble-free arm to facilitate the generation of quiet regions in the centre of the net.

- A spiral form which contains a closed inner ring of bubbles surrounding a bubble-free centre gives additional acoustic protection to the quiet zone at the centre of the net. High-angle rays need only cross two walls to penetrate the centre of the circular bubble net and degrade its quietness; in contrast, they must cross many such interfaces in the spiral net, reflecting at each boundary and attenuating across the width of several bubbly arms.

- Spiral nets need not be generated to such exacting standards as to contain a closed inner ring of bubbles surrounding a bubble-free centre. The circular net requires closure of the circle in order to create a quiet bubble-free region. Of course the inner end of the spiral could close up upon itself, creating in effect a circular bubble net within a spiral one, with a quiet bubble-free region in the centre in which prey are trapped. However spiral nets do not need such accuracy in their construction: they will still work even if there is no complete closure of the bubble layer surrounding a bubble-free centre; and they will still work even if the centre is not bubble-free. This is because the spiral geometry generates new regions, away from the centre but still forming a trap, which are free of bubbles and sound, within the inside edge of the bubble-free arms of the spiral. The ever-closing spiral wall means that, as they progress into the spiral, the reflected rays meet the outer edge of the bubble-free arm of the spiral with ever-decreasing grazing angles (Figure 8(a)), such that the inner edge of the bubble-free arms remains quieter (Figure 8(b)).

- The geometry of Figure 8(b) shows how the whale could speculatively obtain feedback on the performance of the spiral net, since the efficiency of the "wall of sound" could be diagnosed through monitoring the outbound sound as it leaves the spiral.

All this is of course speculation. The authors have no facilities to make measurements in the wild, and whilst it is possible to gain preliminary evidence (Figure 9), this is by no means adequate proof of the theory. Indeed the construction of laboratory bubble nets to test or disprove these theories could provide misleading results. If laboratory experiments are to be conducted, the realism of the model should be critically assessed. For example, it is relatively simple to construct a 1:100 scale model bubble net by submersing expanded polystyrene in water and obtain measured sound fields which at first sight look convincing (Figure 9). Note that this is a spiral with a closed centre, not an open one of the type modelled in Figure 8. Because there is only reflection to consider, propagation in such a net is simple to model numerically [21]. The reason for this is that, in this case, the 'bubble net' was made of expanded polystyrene, a solid matrix containing such a high fraction of gas bubbles frozen in place that it acts as a pressure-release interface underwater. No sound propagated in this scaled-down

'bubble layer', so that the experiment incorporated only the propagation path through the bubble-free arms of the spiral, and did not capture either refraction or propagation within the bubbly arm of the spiral. As a result, the polystyrene model could hardly fail to produce a 'wall of sound' with a quiet interior.

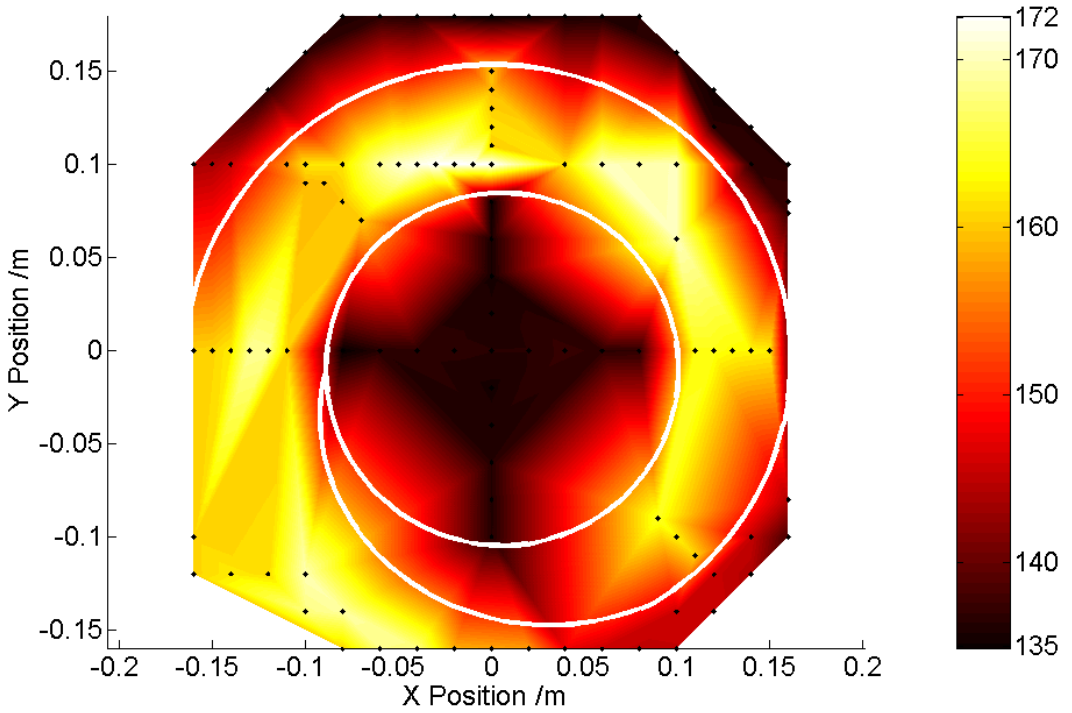

Figure 9.- Measured acoustic field in horizontal plane in demonstration spiral bubble net of expanded polystyrene (1:100 scale, so that the Blacknor Technology sound source projected a 375 kHz pulse into the open end of the spiral). The white line shows plan view position of spiral. Data only exists for the discrete measurement points shown as black dots: between these the colour indicates an interpolation and so, whilst visually appealing, cannot include the zero-pressure at the spiral wall. Colour scale: rms sound pressure level (dB re 1 μPa) at each measurement location, time-averaged over the entire 2 ms window from the start of one pulse to the start of the next (pulses having ~8 μs free-field duration of a 375 kHz basic frequency sinusoid), so that all the reflections within the spiral were included in the calculation. See reference [21] for details.

Why use expanded polystyrene at all for this simple demonstration, rather than proceeding directly to a miniature net of real bubbles? The reason is that the polystyrene only models the impedance mismatch between high-void-fraction bubbly water, and bubble-free water: It is better knowingly to eliminate a key feature (the bubble resonance) from the scale model than it would be to include it with inappropriate scaling.

The problem is that, whilst a physical laboratory model of a net can readily be made to scale the gross dimensions of the net, it is no simple matter to scale the fine structure of the bubble size distribution. The scaling factor used in this experiment is around 1:100. For this, scaling of the gross features is simple: the model net diameter is 0.3 m compared to 30 m in the wild, and the acoustic wavelength is 4 mm compared to the 400 mm chosen to represent the longest wavelength of interest in the net. However such a scaling factor causes problems in generating a suitable bubble population. This is because, whilst the bubble size distribution in the net is not known, it is likely to contain bubbles having radii ranging from centimetres to microns, and this cannot readily be scaled. More importantly, a simple 1:100 scaling is insufficient: as discussed earlier (see Figure 4), for sound to be trapped within the bubble net by refraction, the presence of bubbles must reduce the sound speed, which happens when the bubbles controlling the sound speed are driven at frequencies less than their resonance frequency (i.e. they are driven in stiffness-controlled regime) [1, 3, 4]. The resonance frequency of an air bubble in water varies

roughly inversely with its radius (for bubble greater than, say, ten microns in radius). For insonification at 375 kHz in the scale model, the bubbles which are resonant have radii of less than about 10 microns. Bubbles larger than this would be driven in the inertia-controlled regime [1, 3, 4]. The generation of a bubble net of diameter 30 cm which contained no bubbles larger than about 10 microns radius would be difficult and expensive, involving biomedical contrast agents, electrolysis, chemical reaction, or other alternative [21]. Whilst production of a circle (or even a spiral) of bubbles in a water tank is not too difficult, ensuring that the resonance effects (and therefore sound speed profile) of the bubbly water are scaled appropriately is no simple matter. For this reason, only the reflective element was tested in this preliminary scale model used for Figure 9.

To what extent the humpback whales make use of these acoustical properties is not known, as it is difficult to obtain objective measurements of the sound field, and an assessment of whether whales exploit these features would require a survey which correlated behaviour with acoustics. The geometries of net used have not been surveyed, let alone the relative occurrence of spiral and circular nets. Indeed lunge feeding is seen with other geometries of net [21], but without simultaneous acoustic information, reliable bubble data and behavioural observations, and in sufficient quantity, it is impossible to be certain as to the extent, if any, humpback whales are exploiting these. Visual impressions by observers of the shape of bubble nets, and the distributions of bubbles within it, may not accurately reflect the way the acoustic field 'sees' the net. This is because whilst large bubbles catch the eye and rise quickly under buoyancy to the surface, where they are seen, the greater acoustical effect may be generated by clouds of smaller bubbles which persist for long times in the water column, and (from our experience in test tanks) can be much more difficult to see. It may be that the formation of spirals nets is simply the by-product of some behaviour designed to achieve another purpose, such as efficient motion during the formation of the net, just as the shape of natural spirals whose response to pressure perturbations is key to their function (e.g. the cochlea, the nautilus shell) has been attributed to expedient (if the perhaps mundane) explanations such as efficient packing. However the remarkable effect of the spiral on fields propagating along it (such as the ever-decreasing grazing angle which will, if the spiral is sufficiently long, eventually generate wall-hugging surface waves; the robustness to the particulars of the entry; and the possibility of feedback from back-propagating fields) are suggestive of possibilities that should be explored.

THE BUBBLE NETS OF ODONTOCETI

The bubble nets discussed so far in this paper were generated by humpback whales, and the associated feeding calls contained energy at frequencies less than 4 kHz. As such, the acoustical interaction between the two (which, it is postulated, might be a deliberate endeavour to aid feeding) is relatively simple: from Figure 4, assuming a bubble size distribution resembling that found at sea, the bubbles at these frequencies will tend to reduce the sound field in a relatively stable manner (Figure 4(b)), and the extra attenuation produced by the bubble presence will be lower than at other frequencies (the absolute value depending on he void fraction).

The acoustics of odontoceti in bubbly water are a different matter altogether, because whilst there is no firm evidence to date of humpback whales exploiting such >30 kHz frequencies, *odontoceti* are well-known for using echolocation frequencies of tens of kHz or even in excess of 100 kHz [29, 30]. Furthermore, the information requirements for echolocation of prey are likely to be much greater than those of forming a 'wall of sound'.

Nevertheless certain species of dolphins and porpoises have renowned abilities for operating in the shallow coastal waters and biologically active rivers where bubbles persist, and indeed some species of river odontoceti have effectively no visual acuity. Such creatures no doubt have a range of advantageous features to assist in the detection, localization and characterisation of targets by sonar, such as their 'platform' capability. That is to say, their sonar is mounted on a body which can move rapidly through the environment and expose a target to a sequence of sonar signals in quick succession form a range of angles and viewpoints, and with the capability to change the distance and orientation to target with rapidity and control.

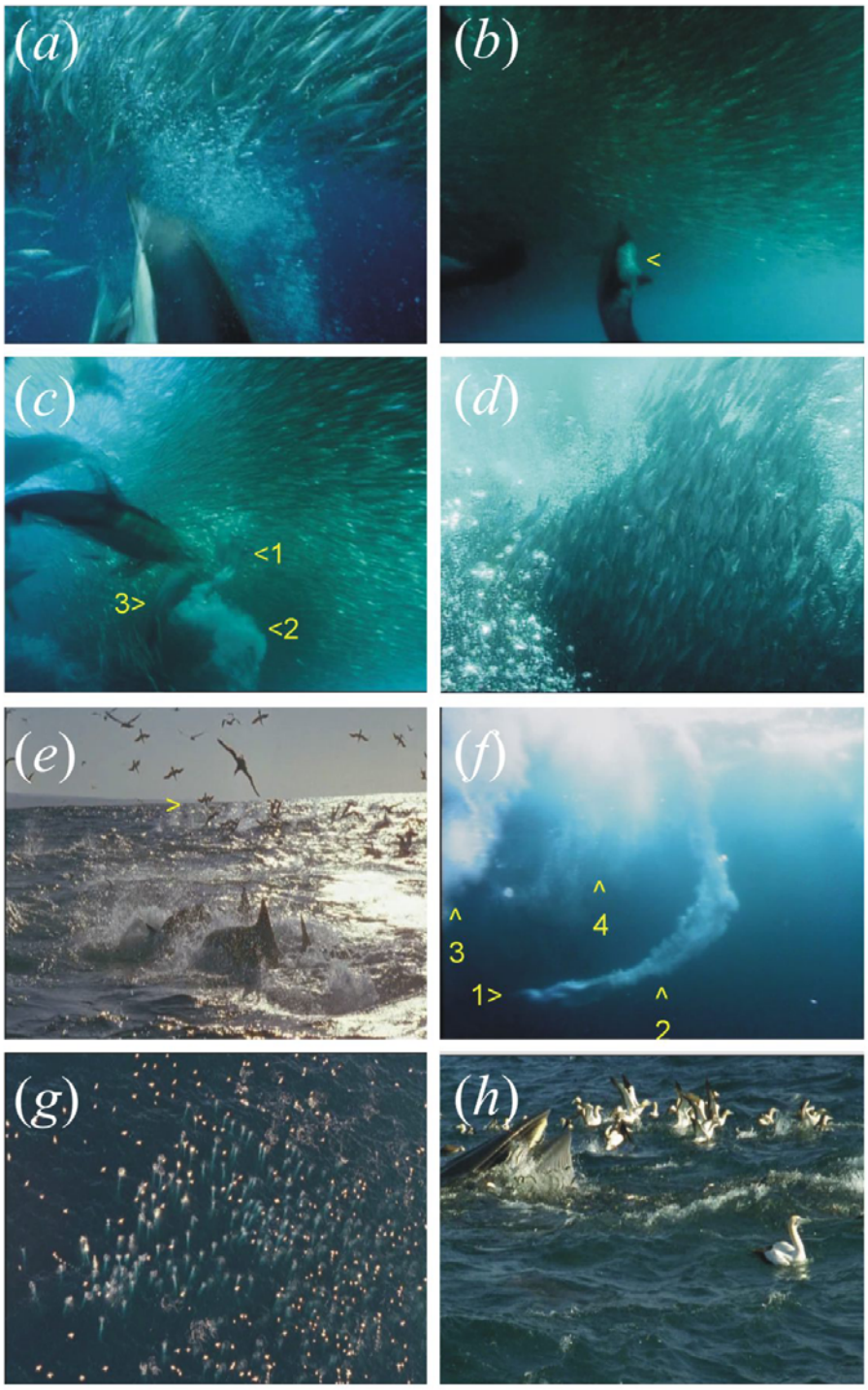

Figure 10. (a) Common dolphins herd sardines with bubble nets. (b) A dolphin starts to release a cloud of bubbles (arrowed) from its blowhole. A moment later (c) this dolphin (1) swims on, leaving behind the expanding cloud (2). Other dolphins (including the individual labeled '3') enter the frame. (d) The sardines school within a wall of bubbles that they are reluctant to cross, whilst (e) gannets dive into the sardine shoal to feed (arrowed). (f) On diving, a gannet (1) entrains a bubble plume (2). Plumes a few seconds old (3, with an older 4) have spread. (g) An aerial view shows hundreds of tight bubble plumes beneath airborne gannets. (h) A Bryde's Whale joins the feed. It surfaces with open mouth, which it then closes, sardines spilling from it. Images copyright of The Blue Planet (BBC) and reproduced with permission. The accompanying book to the series is Byatt *et al*. [31].

Given their acoustic potency, bubbles constitute a key feature which compromises active sonar in such shallow water environment. However some species of odontoceti not only tolerate the bubbles of coastal waters, but at times generate them. The filming associated with Byatt *et al.* [31] detailed bubble nets produced by dolphins (Figure 10(a)-(d)). It also showed bubble plumes generated by gannets (Figure 10(e)-(g)) diving into a shoal of sardines which dolphins have herded to the sea surface. These plumes will no doubt complicate an underwater sound field already populated by the calls and bubble nets of dolphins, and the entrainment noise of the gannet bubble plumes, and could further stimulate the sardines to school. Gannets, dolphins, sharks and whales etc. (Figure 10(h)) all benefit from this, although to what extent this is intentional is unknown.

This paper will explore the possibility that some species might be deliberately generating and exploiting multiple pulses to ameliorate the clutter generated by bubbles in the water column. The hypothesis is not biomimetic, in that no attempt was made to mimic signals generated by natural creatures. The proposal was inspired when the first author saw the BBC video footage from which Figure 10 has been generated, when he was unaware that some species of ondontoceti might generate multiple pulses. That footage shows dolphins deliberately generating bubble nets in which to hunt. No man-made sonar would function in such bubble clouds. In response to logical conclusion that these dolphins either (i) were deliberately impairing their sonar when they generated such nets to hunt, or (ii) had evolved a sonar system which could detect targets in such bubble clouds, he proposed that they might be exploiting multiple pulses with inverted phases [1,5]. These references contained a proposed thought-experiment (illustrated in Figure 11). In this, one wishes to use sonar to detect a linear scatterer, given that there is a bubble cloud in the propagation path. Such a linear scatterer might be a fish, with or without a swim bladder (which at sufficiently high frequencies would behave linearly) within a dolphin bubble net. If amplitude of the insonifying field were to be high enough to generate a nonlinear response, it might be possible to enhance scatter from the mine, whilst simultaneously suppressing it from the bubbles. Consider an insonifying field consisting of two high amplitude pulses, one having reverse polarity with respect to the other (Figure 11, top line). Linear reflection from the linearly scattering body (which we shall call the 'solid') is shown in b(i). The bubble generates nonlinear radial excursions (Figure 11 a(i)) and emits a corresponding pressure field (Figure 11 a(i)) (the relevant time histories can readily be calculated [17]). Normal sonar would not be able to detect the signal from the solid (Figure 11 b(i)), as it is swamped by that from the bubbles (Figure 11 a(ii)).

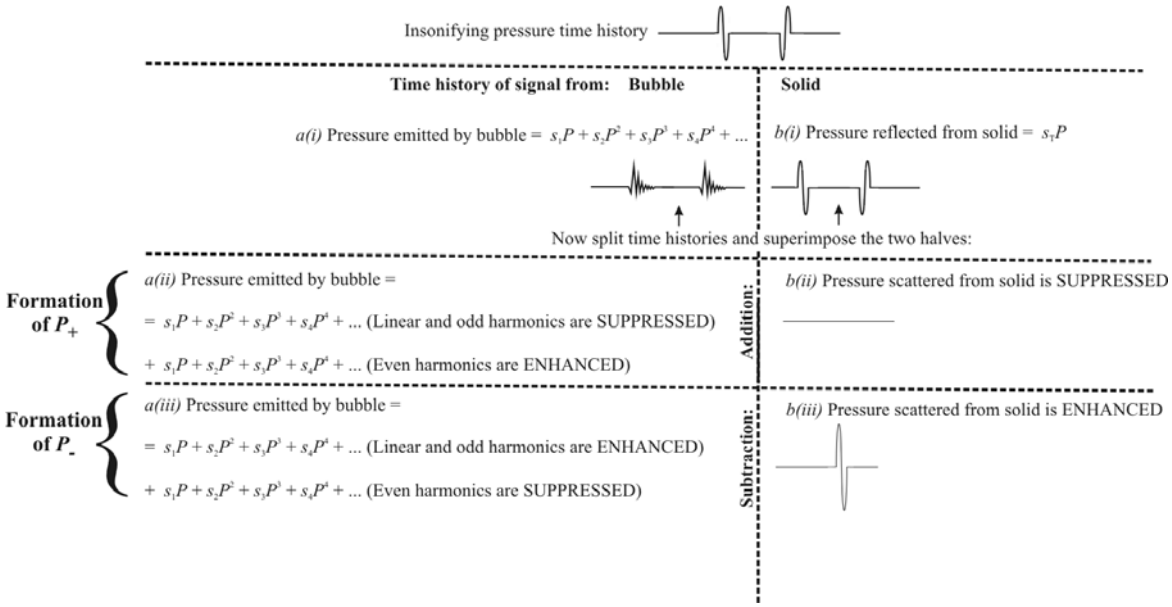

Figure 11.- Schematic of the formation of P_+ and P_-

If however the returned time histories are split in the middle and combined to make a time history half as long, enhancement and suppression occurs. If the two halves of the returned signals are added, the scattering from the bubble is enhanced (Figure 11 a(iii) and a(iv)), whilst

the scatter from linear scatterers (such as the solid) is suppressed (Figure 11 b(ii)). This could be used to enhance the scatter from contrast agents [32, 33]. If however the two halves of each returned signal are subtracted from one another, the scattering from the bubbles is suppressed (Figure 11 a(v) and a(vi)) whilst the reflections from the solid body are doubled (Figure 11 b(iii)).

Simulations have been undertaken to test whether the proposed Twin Inverted Pulse Sonar (TWIPS) could reveal a linearly scattering object that hidden to conventional sonar within a bubble cloud [6, 28, 34, 35]. The simulation incorporated three basic elements: an insonifying wavetrain (Figure 12(a), a bubble cloud and a target (Figure 12(b)). When present, the target is located at the centre of the cloud and assumed to scatter linearly. The simulation uses target strengths of -20 and -25 dB (the latter would be equivalent to Atlantic cod (*Gadus morhua*) broadside to an acoustic beam operating in the frequency regime of interest). The bubble cloud is assumed to be a sphere of radius 1 m, containing around 35 million bubbles following the population size distribution as measured at sea [36], such that the void fractions (the ratio of the volume of gas within a cloud to the total volume occupied by the cloud) on the order of 10^{-7} (i.e. 10^{-5} %).

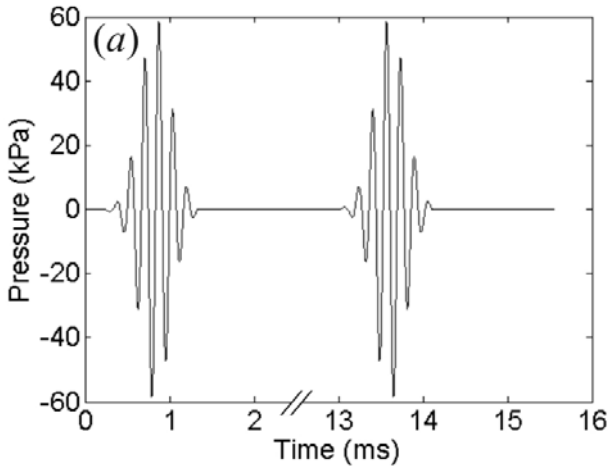

(a)

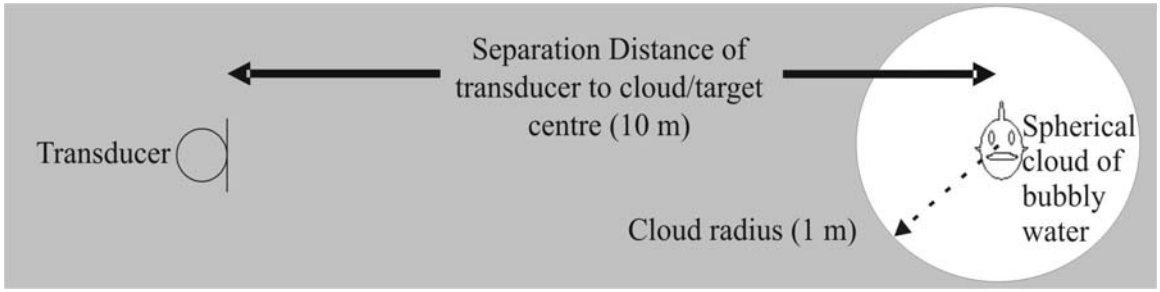

(b)

Figure 12. (a) The wavetrains used to insonify the marine environment in the particular implementation of TWIPS used in the simulation (b) Diagram of simulation geometry for transducer, target and spherical bubble cloud (see [9, 35] for details).

The cloud is dynamic, evolving as a consequence of turbulence, buoyancy etc. [1, 17], although the average number and spatial distribution of bubbles is constant. The insonifying wavetrain is shown in Figure 12(a). It consists of two pulses, identical except that the second (the 'negative' pulse) has opposite polarity to the first (the 'positive' pulse).

The scattered pressure for monostatic operation was calculated from a region of seawater containing spherical cloud of bubbles of radius 1 m, centred on the target (which was at range 10 m from the transducer) (Figure 12(b)), in order to determine which sonar system could detect whether a target was present in the cloud.

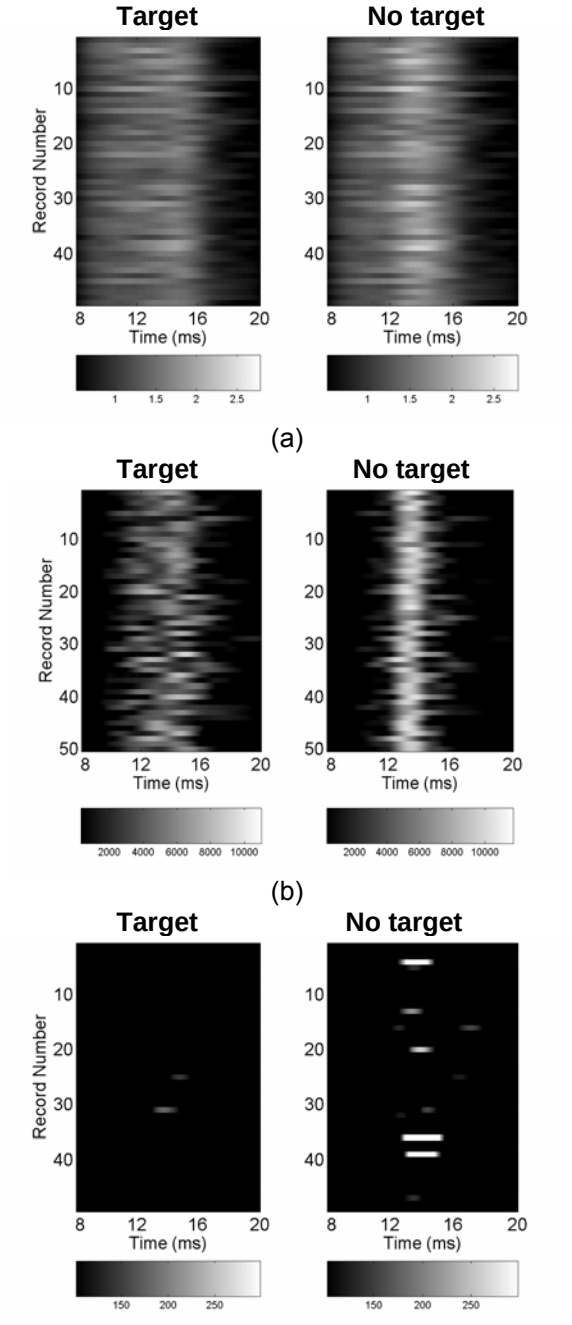

Figure 13. Fifty pulse pairs were projected at the cloud, spaced at intervals of 10 ms, and the echoes processed using (a) conventional sonar deconvolution techniques, (b) TWIPS1 and (c) TWIPS2b. The left plot in each panel shows the case when there is no target present, and the right plot shows the case when a target is inserted at the cloud centre (TS = -20 dB). The cloud, of 1 m radius, contains 35 million bubbles, and evolves appropriately between each ping, as described earlier (Fig. 11). (a) A single average was formed from the two pulses that make up each pulse pair, such that 50 averages are available for plotting. Each average was plotted as a time history on a one-dimensional line, with a greyscale such that the amplitude of the signal at the corresponding moment in the time history was displayed. These processed echo time histories were then stacked, one above each other, to form an image. (b) TWIPS1 processing of the 50 pulse pairs (no averaging) are displayed similarly, by stacking the consecutive grey-scale time series one above the other. were projected at the cloud, spaced at intervals of 10 ms. The TWIPS1 processed echoes were plotted, each as a time history on a one-dimensional line, as in (a). (c) TWIPS2b processing is used (no averaging) and the image displayed as in (b). See Leighton *et al*. [6, 35] for details.

In current sonar signal processing, averaging and correlation are used to amplify signals which are consistently found in the same temporal location. Experience has shown that this technique does not yield useful results in the complex, dynamic acoustic environment encountered in a bubble cloud. For the same set of incident pulses, conventional sonar processing was compared with two forms of TWIPS: TWIPS1 and TWIPS2b. TWIPS covers a range of processing techniques, with different capabilities. All are designed to enhance contrast of targets in bubble clouds, both by increasing the scatter from the target and, very importantly, at the same time suppressing the signals from the bubbles. TWIPS1 is designed always to enhance target contrast, producing a reliable enhancement with every ping. TWIPS2b gives much greater contrast enhancements, but not with every ping: the particular form demonstrated here 'glints' on about 10% of pings. However the contrast enhancement is much greater than occurs with TWIPS1. It is particularly useful for sources that have the luxury of insonifying a region with multiple pings.

For conventional sonar (Figure 13(a)), TWIPS1 (Figure 13(b)) and TWIPS2b (Fig. 13(c)), 50 pulse pairs were projected at the cloud, spaced at intervals of 10 ms. The processed echoes were then stacked, one above each other, to form an image. As a stationary feature in the display, detection of the target in every ping would correspond to the observation of a vertical white line which is visible when the target is present, but absent from the corresponding sonar plot when the target is absent.

The left hand plots in the individual panels of Figure 13 correspond to the cloud when there is no target present, and the right hand plots of each panel in Figure 13 correspond to the bubble cloud when the target (TS = -20 dB) is present. In comparing the results, resist the temptation to compare against each other the 'target present' plots in (a)-(c). Rather, consider the judgements made by sonar operators: Recalling that the same echo can be processed by conventional and TWIPS techniques simultaneously, consider the difference between the left and right plots in each panel, and ask whether a sonar operator or dolphin or porpoise could tell, from the left panel, that a target was absent; and from the right, whether there is a possible target to investigate.

Standard sonar processing fails to detect the target: There is insufficient difference between the two plots in Figure 13(a) because scatter from the bubbles masks the presence of the target. TWIPS1 detects the target on almost every occasion, such that there is a vertical line on the right of Fig. 13(b) compared to the plot on the left (where, importantly, it has suppressed the bubble signal). As stated earlier, TWIPS2 is designed to work spectacularly for about 10% of pings. This feature is shown in Figure 13(c), in that for some pings it fails to detect the target is present at all. However when it does detect one, the amplitude is very high (see plot on the right); when the target is not present (left hand plot), it rarely delivers a high amplitude return, very effectively suppressing the returned signal. The plots all have a linear greyscale and no thresholding has been applied.

Following simulations which indicated that the TWIPS procedure would be viable [6, 34, 35], the authors undertook experiments [35, 37] to verify these predictions. In the proof-of-principle experiments (Figure 14), the bubble clouds had dimensions of O(1 m). Efforts were made to ensure that the clouds contained bubbles ranging in radii resembling that found in the ocean [38]. It should be pointed out that (i) the efficacy of TWIPS decreases as the bubble size distribution increases, so that proof that it works with such a wide ocean-like distribution is important; and (ii) the characteristics of the bubble cloud were only measured after the successful deployment of TWIPS reported here: this was not a case of using *a priori* information on the bubble cloud in order to optimise the insonification signal or the processing.

Figure 14 shows the component of the experiment which comprises the equipment use to detect the target. The bubble generation system is shown in Figure 15 (the two are drawn separately for clarity, although they were deployed at the same time).

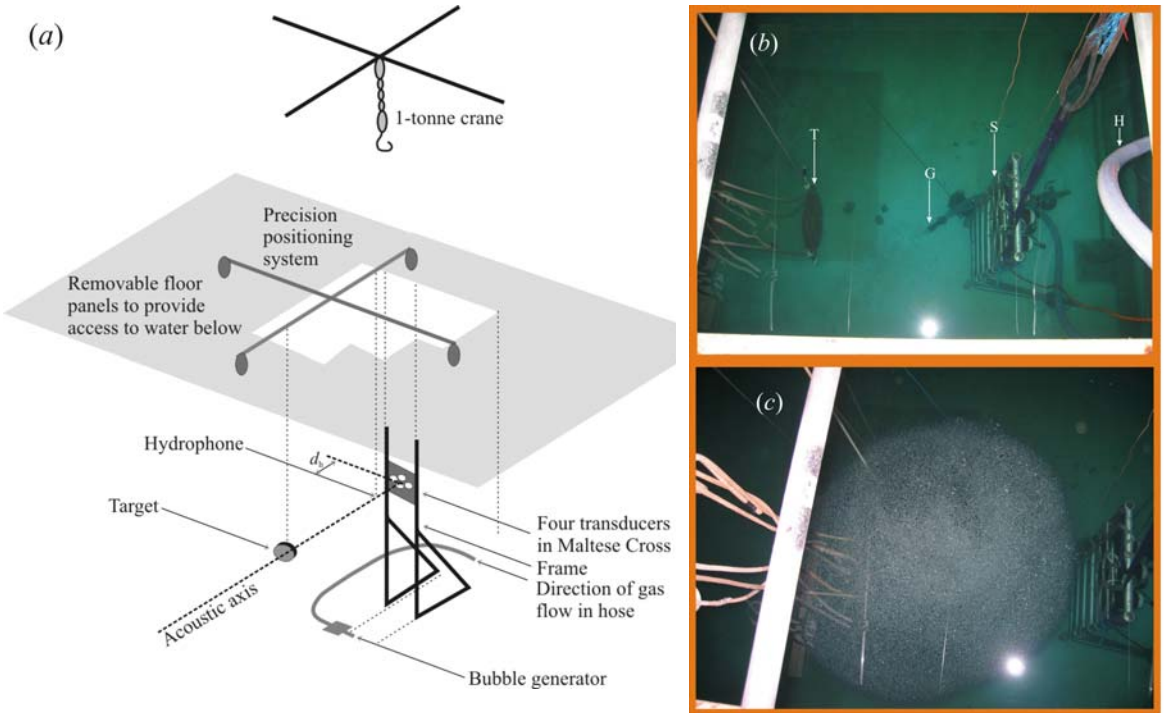

Figure 14.- (a) Schematic of proof-of-principle TWIPS experiment. Below the floor (shown shaded) is an underground water tank, 8 m × 8 m × 5 m deep. A rigid frame holds 4 transducers in a Maltese Cross, A hydrophone and a target are aligned on the horizontal acoustic axis, the hydrophone behind d_h=0.40 m in front of the source faceplate . (b) Photograph looking down into the water. Target (T) is 2.00 m from source (S). Hose (H) feeds the bubble distribution unit (G). (c) The same perspective as (b), but now with bubble cloud. Target detection experiments with this cloud are detailed in reference [35]. The cloud used for the target detection results presented in this paper is shown in Figure 19.

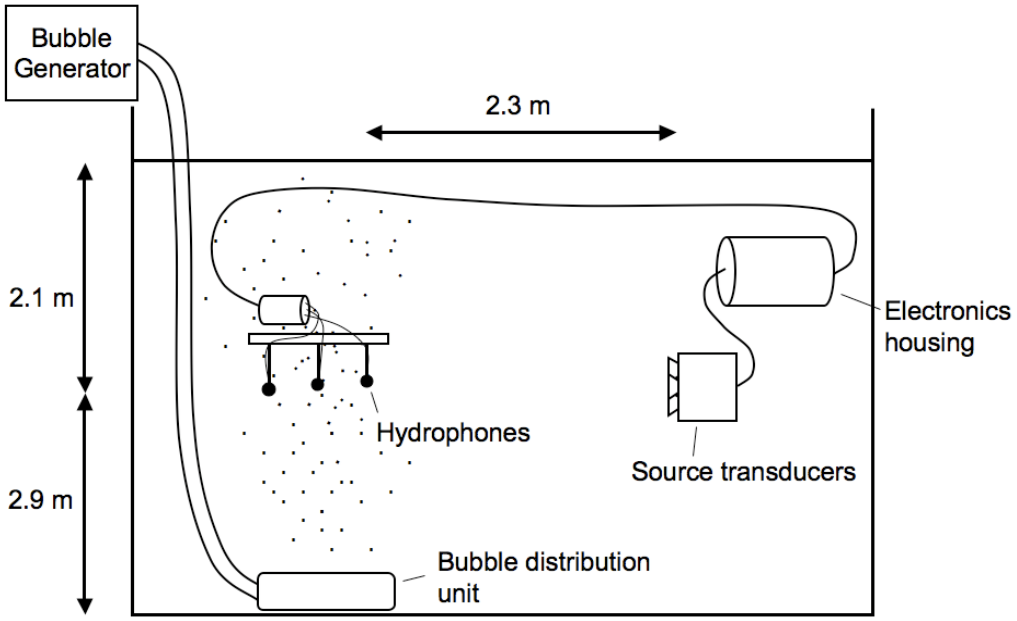

Figure 15.- Bubble generation and measurement components of the tank tests which took place in the 8 × 8 × 5 m^3 AB Wood tank alongside the target detection tests of Figure 14. The hydrophone spacing is 0.31 m. From Coles and Leighton [38].

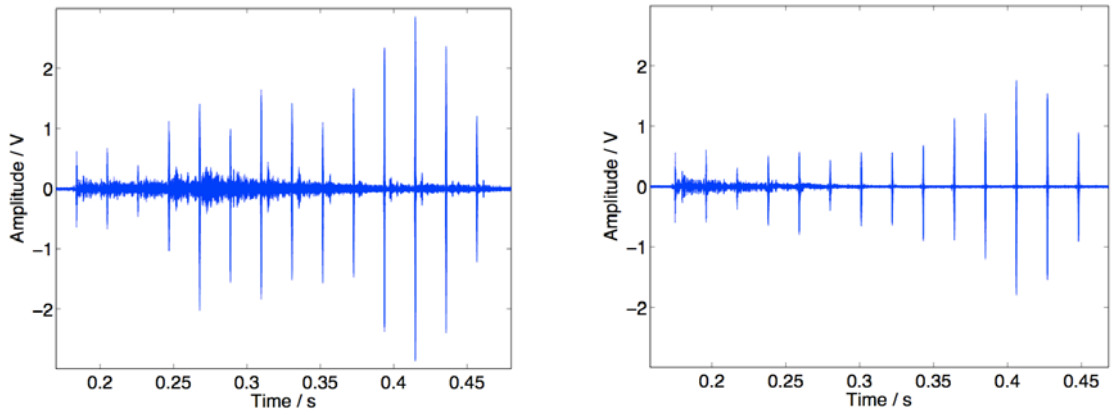

(a) *(b)*

Figure 16.- The signals used to characterise the bubble population (not for target detection). (a) The pulse train measured at the second hydrophone with no bubbles present. (b) The increased attenuation at the same hydrophone when bubbles (shown in Figure 19(b)) are present. From Coles and Leighton [38].

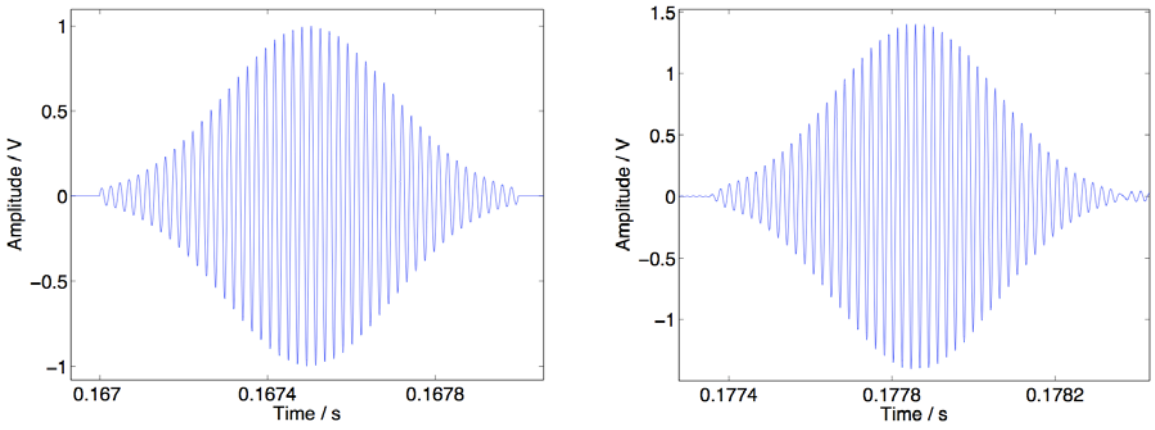

(a) *(b)*

Figure 17.- Components of the signals used to characterise the bubble population (not for target detection). (a) The outgoing 46 kHz pulse signal that was transmitted to the power amplifiers prior to output into the water. (b) The same pulse as measured by the hydrophones in bubble-free conditions. From Coles and Leighton [38].

The outgoing signal was a train of 14 pulses, varying in frequency from 3 to 197 kHz (Figure 16). These were generated by a data acquisition card, and matched via the power amplifiers and transducers such that the pulses in the water followed the waveforms supplied by the data acquisition card with high fidelity (Figure 17) [38]. This high fidelity was designed by Paul Doust of Blacknor Technology. The hydrophones used were D/140 broadband hydrophones. The 3 to 197 kHz frequency range allowed measurements for bubble sizes ranging from 17 – 1107 μm in radius to be carried out. Each pulse was 1 ms long, short enough so the received signal was not to be affected by any multi-path reflections. There was a 20 ms off-time between pulses to allow for bubble ring-down. The time between pulse trains was approximately 1 second, dictated by the speed at which the computer could save the data files. The attenuation between the hydrophones at each frequency was measured. To generate bubbles, a Venturi system was used (Figure 15). The water in the 'bubble generator' shown in the top left corner of Figure 15 is filled with a population of very small bubbles (Figure 18), through Venturi action. This bubbly water then pumped through the hose (labelled H in Figure 14(b), and shown on the left of Figure 15) to the base of the main tank, where the various 'bubble distribution unit' (labelled 'G' in Figure 14(b), and shown in Figure 15) are placed. These modify the bubble size distribution to provide the population required (such as the spherical cloud of Figure 14(c), or the more homogeneous distributions shown in Figure 19.

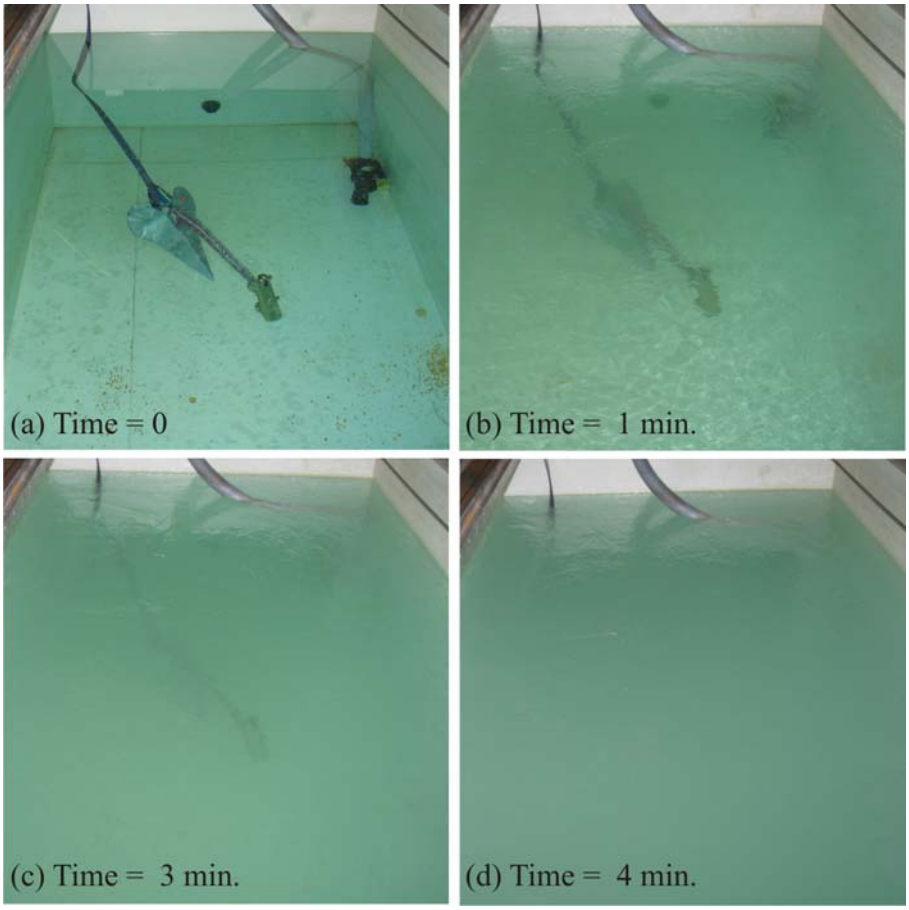

Figure 18.- The water in the bubble generator shown at the top left corner of figure 15. The images corresponding to times of (a) 0, (b) 1 min., (c) 3 min and (d) 4 min. after activation of the generator. They show the system filling a tank of normal fresh water (measuring 1.5 m x 2.5 m x 1.5 m) with a dense cloud of minute bubbles, without the production of large bubbles. As a result, the initially clear water turns milky white, obscuring from view the Delta 22 anchor which lies under 1.5 meters of water and measures 27.375 inches end-to end and a maximum of 12.25 inches between the fluke tips. No chemicals were used.

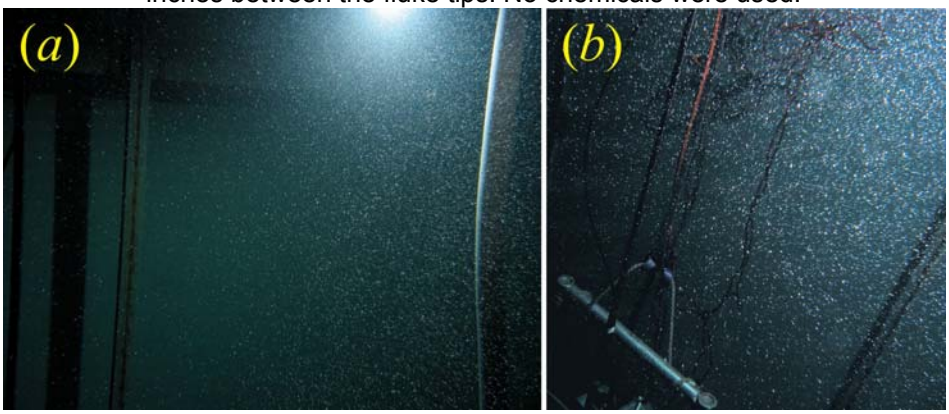

Figure 19.- (a) This image shows the bubble cloud used during one TWIPS test. The section of wall visible in the background of the photo measures ~3.3 m x 2.5 m, and is at a distance of 3 m from the camera location. The bubble cloud is distributed into the water column by a diffuser located halfway between the camera and the wall. The hose (white, at right), is 5 cm in diameter, and is along the approximate centreline of the cloud, at a distance of 1.5 m from the camera location. (b) Photograph from the top of the water column, showing the scaffolding bar at the top of the frame which holds the source. That bar is at a depth in the water of 2.03 m, and its length is 0.8 m.

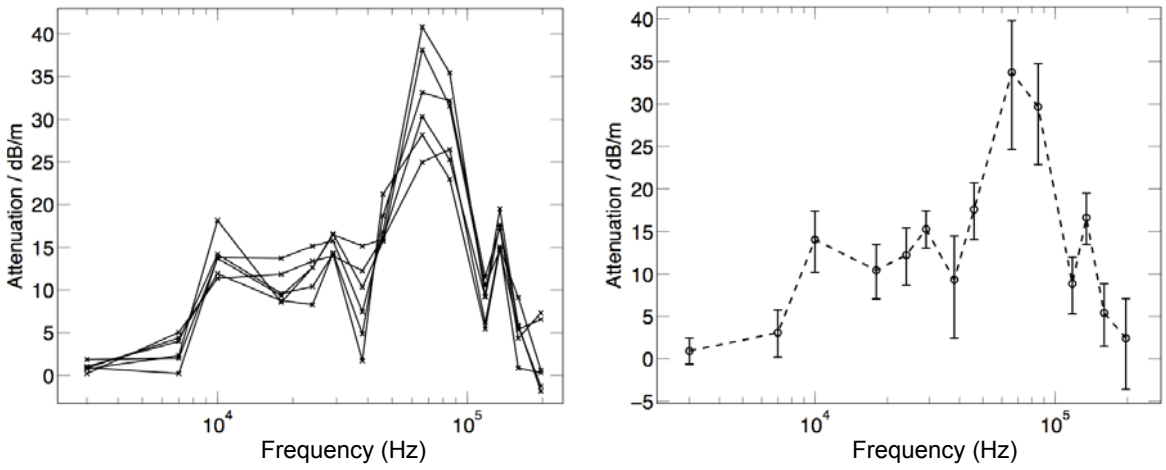

(a) (b)

Figure 20.- Data for the bubble population of Figure 19(b). (a) The additional attenuation due to bubbles between the 1st and 3rd hydrophones, which were at a distance of 0.62 metres apart. The figure shows 6 separate readings, spaced approximately 1 second apart. (b) The mean of the 6 values shown in (a) (calculated from linear pressure data, not dBs). The error bars represent 1 standard deviation from the mean of the 6 values and also take into account the uncertainty of the hydrophone calibrations. From Coles and Leighton [38].

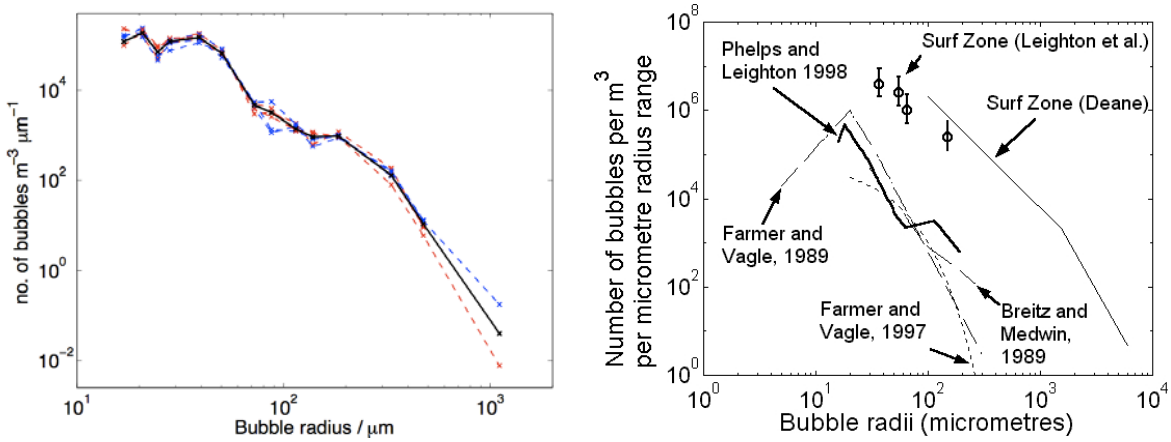

(a) (b)

Figure 21.- (a) Bubble size distributions as calculated from measured attenuations of Figure 20. The bold black line shows the 6 second average population, the dashed lines show the six individual populations which make up the average. From Coles and Leighton [38]. (b) Previously measured oceanic bubble populations (taken from [2], where the sources are listed in full).

The measured acoustic attenuation (Figure 20) was inverted to estimate the bubble size distribution and void fraction generated by this system (Figure 21(a)), and check that, as required, it was similar to the characteristics of oceanic bubble populations (Figure 21(b))

An example of the measured attenuation due to bubbles is shown in Figure 20. The error bars in Figure 20 (b) are at times large because of the fluctuating nature of the bubble cloud as it rises through the tank. The mean attenuation data from 6 readings were inverted to obtain bubble size distributions (Figure 21 (a)) [38]. As would be expected from Figure 24, very few bubbles were found at the largest bubble radius (1107 μm). The distribution measured in the tank (Figure 21(a)) is very similar in gradient and magnitude to historical measurements (Figure 21(b)). Comparison of Figures 20 and 21 with Figure 4 confirms that the bubble population in the test tank resembles that founding the ocean.

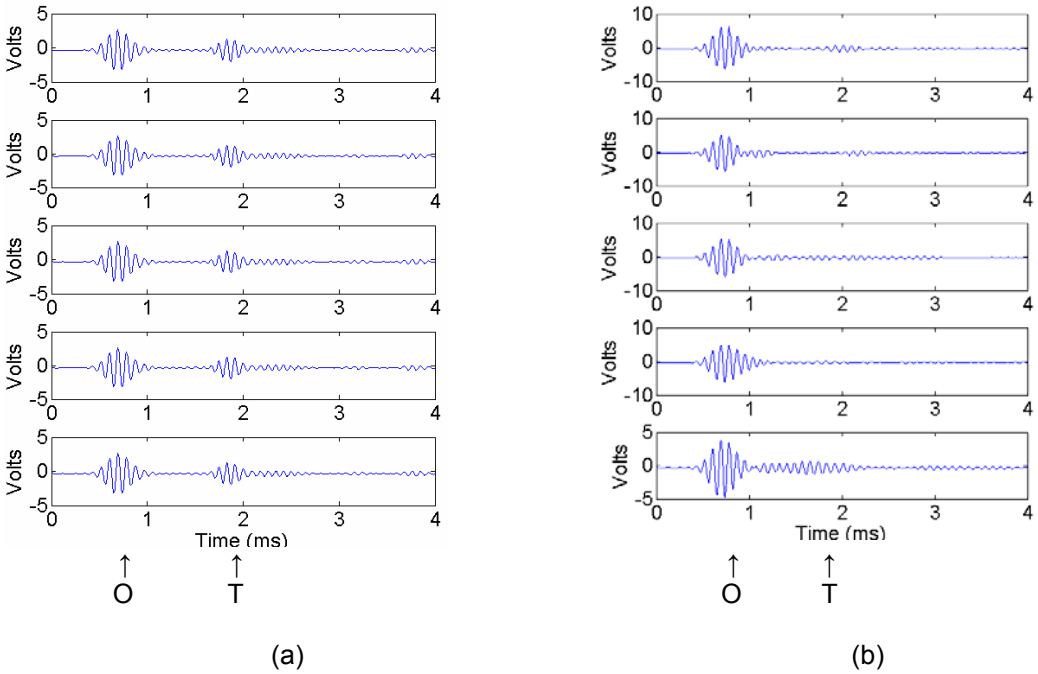

Figure 22.- A sequence of consecutive signals from the hydrophone of Fig. 1(a), arbitrarily selected for display. In (a) no bubbles are present. The first of the outgoing twin pulses (O, propagating out from source to target) is shown, followed around 1 ms later by the returning echo from the target (T, which propagates back from target to source). The second in the pair of TWIPS pulses is sent out 20 ms afterwards, and produces corresponding echoes. In (b) bubbles are present (Figure 19(b) and 21(a)). Although the outgoing pulse is relatively stable, there is significant clutter from the bubbles and the signal from the target is attenuated.

The outgoing waveform consists of two pulses sent out 20 ms apart, the second having reversed polarity with respect to the first. The waveform prior to 1 ms in Fig 22(a) shows the first of this pair of pulses in the absence of bubbles, under which conditions it has a temporal peak pressure amplitude (0-peak) of around 25 kPa at 1 m from the source, and 15 kPa at the target. The target is a steel disc of diameter 415 mm and thickness 50 mm, and at range 2 m from the source. Its calculated target strength is -10 dB.

Figure 22 shows a sequence of hydrophone records, arbitrarily chosen, which demonstrate the effect which the presence of bubbles have on the detectability of the target. When 10 such returns (arbitrarily chosen) are stacked (Figure 23), the ability of TWIPS to detect the target when it is hidden by bubbles is clearly demonstrated. The agreement between the experiment, and the simulations made in 2005 before any experiment was planned [6, 28], is spectacular. An example of this is found in the intermittent manner in which TWIPS2a detects the target. This feature was predicted in the simulations [6, 34], and is one that could be offset in human or dolphin sonar by the use of a train of clicks: note that no fitting or adjustment parameters have been used with this data.

The implications of verifying the simulations of TWIPS working by providing an operational demonstration in the laboratory are significant. There is need for a method which allows active sonar to operate in shallow coastal waters (the littoral zone), a problem which, despite significant investment, has not previously been solved. Quoting Rear Admiral W.E. Landay (Chief of Naval Research, Marine Corps for Science and Technology). O. Kreisher wrote *'The explosive ordnance disposal divers and the marine mammals run counter to the drive to get people out of the minefields, Landay said, but they provide "so much flexible capability" that they are likely to remain. The divers and the mammals work mainly in very shallow water and the surf zone, which "continues to be the most challenging environment" for mine warfare, he said'* [39]. If TWIPS could be made operational at sea, this would be a step towards replacing the current need of the US Navy to deploy odontoceti, and increase security for navy personnel

and equipment in shallow bubbly waters. Such innovations are required since military operations (e.g. mine detection, landings, and the protection of harbours and shipping lanes for military, commercial and aid craft) cannot rely on the decades of sonar experience built up for deep water applications during the Cold War. Such advances in sonar are also required because of the increasing use of sonar in shallow waters (e.g. for fisheries, surveying, and to cope with bottom sensing in increasingly-crowded and wake-filled waters by commercial and leisure craft). TWIPS sonar not only enhances the scatter from the target, but suppresses the clutter from the bubbles. As such it opens the door for then employing further processing techniques, such as target recognition imaging or through the exploitation of target resonances (for which the pulses of Figures 12(a) and 22(a) would be well suited).

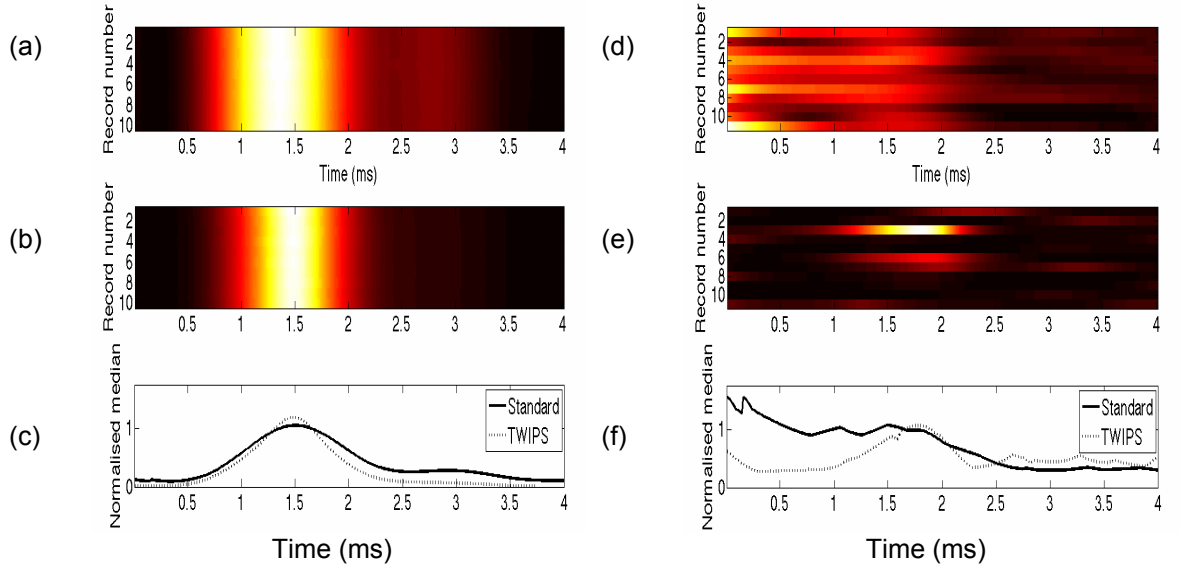

Figure 23: For both standard sonar (Panel (a) & (d) and TWIPS2a (Panel (b) & (e)) (as defined in reference [35]), hydrophone signals of the type shown in Fig. 2 are stacked consecutively one above the other, with start time t=0 chosen to be after the outgoing pulse (labelled O in Fig. 2) has passed over the hydrophone. Panels (a)-(c) refer to measurements taken in the absence of bubbles. The target is clearly visible at t~1.4 ms to both standard sonar (Panel (a)) and TWIPS2a (Panel (b)). When the normalised median of these 10 signals is calculated in (c), both standard sonar and TWIPS2a clearly show the target. Panels (d)-(f) shows the equivalent plot as for (a)-(c), but now with the introduction of a bubble population [38]. In (d) standard sonar can no longer see the target: the image is dominated by scatter from the bubble cloud. In (e) the scatter from the bubble cloud has been suppressed, and that from the target has been enhanced, such that the target is clearly visible. In (f) TWIPS2a clearly shows the presence of the target (note the suppression of the echoes from the bubbles), whilst standard sonar does not.

There are also implications for electromagnetic radiation in the ability to suppress unwanted nonlinear clutter (such as the 'rusty bolt' effect in radomes) or enhance it (to detect covert circuitry with radar, or to detect combustion products with LIDAR). There is a range of commercial and security applications (for example with optoelectronics and THz radiation) [35].

Recall that the impetus for this problem came from the search for a possible way of obtaining sonar enhancement in bubbly waters, given that ondontoceti were observed to function in such waters [1, 5]. The object was not to mimic the sonar of ondotoceti. However having proven that TWIPS works in the laboratory, it is logical therefore to speculate whether odontoceti make use of this technique. Following the proposal of TWIPS [1, 5] and the success of the simulations [6, 34], conversations between the authors and members of the cetacean research community revealed that multiple pulses are indeed sometimes observed from *odontocete*. Whilst under very still conditions a reflection from the water/air interface could produce a phase-inverted signal, a search of the records by the authors revealed that six species of dolphins and porpoises (all belonging to the genera *Cephalarynchus* and *Phocoena*) in fact have been

reported to create multiple pulses deliberately [40-42]. These species are listed in Table 1. The primary habitats for all members of these genera are shallow waters - the same waters for which TWIPS was invented as a sonar solution.

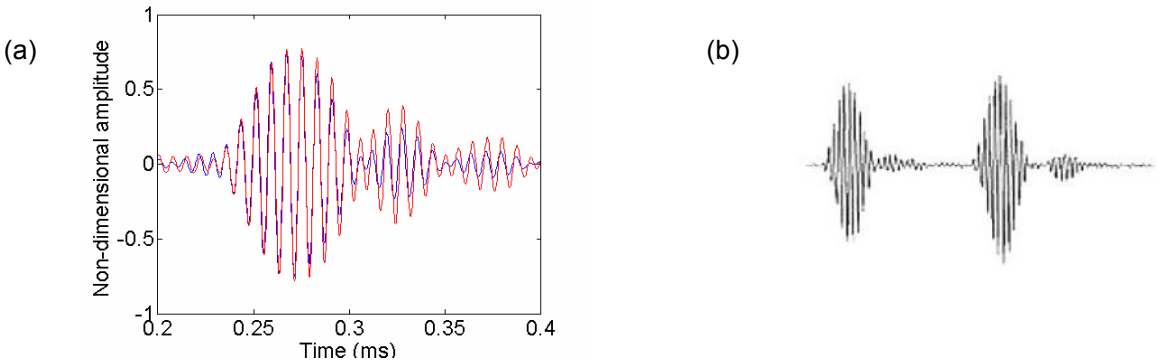

Figure 24.- (a) Two closely-spaced pulses from Hector's dolphin have been overlaid, having first inverted the 2nd pulse (shown in red). This then closely overlays the 1st pulse (shown in blue) indicating that the 2nd pulse was originally phase-inverted with respect to the 1st. However this is not conclusive evidence, because the data had to be oversampled by a factor of 10 because most of the energy within the signal falls just below the folding frequency. (Raw data courtesy Steve Dawson, University of Otago, processed by the authors). (b) Emission by Yangtze finless porpoise (reproduced from reference [43]). Axes not available. The 2nd wavepacket occurs ~300 μs after onset of 1st. Data-limited analysis suggests 2nd packet is inverted with respect to 1st.

Pre-existing acoustic data for these mammals is scarce and, as a result of the wide bandwidth and high frequencies of the sounds they produce, it is often not sampled at a sufficiently high frequency to allow accurate phase analysis. Nevertheless phase analysis by the authors of recordings of Hector's dolphin (supplied to them by Dr Steve Dawson of the University of Otago, Dunedin, New Zealand) strongly suggests that this species is capable of deliberately generating phase inverted pulses (Figure 24(a)).

Furthermore, the twin pulses detected from the Finless Porpoise were also shown to be phase inverted by Li *et al.* [43] (Figure 24(*b*)). However those investigators assumed that the Finless Porpoises themselves did not generate twin inverted pulses, but rather that they generated a single pulse and that second pulse was the result of a reflection of the initial pulse from the air/water interface. Dawson and Thorpe [42] point out that while surface reflections may sometimes dominate the acoustic response, there have been many cases recorded where the multi-pulse structure (the inter-pulse timing and relative amplitude) does not vary considerably. In such cases, he argues, this would indicate that the multi-pulse is in fact emanating directly from the moving animal, as the structure of a signal inclusive of significant surface reflections would alter as the animal moved closer or further away from the hydrophone.

Convincing historical evidence which would suggest that the interpretation of multiple pulses as surface reflections is incorrect, is found in a 1966 paper by Medwin [44], who addressed the surface reflections from a wind driven surface. This paper showed reasonable agreement between Kirchhoff scattering theory and experiment. Medwin fixed an up-looking send/receive transducer on the bottom of the tank, and played 8 tones 20 times. The tones used were linearly spaced from 21.5 kHz to 194 kHz. The tank surface was maintained at a near-constant roughness throughout the course of the experiment, so that, in dimensional terms, the higher frequency measurements effectively modelled rougher seas. For anything more than superficial roughness (e.g. as the wavelength approaches the median size of surface disturbance), it becomes very difficult to obtain reflections of amplitude greater than about half that obtained when the surface was smooth and flat.

One coastal dolphin which is not listed in Table 1, but which belongs to the genera *Cephalarynchus*, is Heaviside's dolphin (*Cephalorhynchus heavisidii*). This is because the authors are unaware of any acoustic data in the public domain on this species, which is confined to coastal Africa. However, given the close evolutionary ties between Heaviside's

dolphin and the other dolphins of its genus [45] and the relative similarities of their limited habitats, we propose that acoustic measurements of Heaviside's dolphin could reveal the presence of multiple phase-reversed pulses.

Table 1: Species for which there is tentative evidence for the deliberate use of multiple pulses for sonar in shallow water, with sources for that evidence referenced. Note: Awbrey *et al*. [47] made the first high frequency recordings of Dall's porpoise, but the authors of this paper were unable to obtain this report.

Species	**Primary Habitat**	**Ref.**
Dall's porpoise, *Phocoena dalli*	Near-shore, warm temperate to sub-arctic waters of the Northern Pacific Ocean.	[46, 47]
Harbour porpoise, *Phocoena phocoena*	Coastal waters of subarctic & cool temperate North Atlantic & North Pacific. Often inshore.	[41]
Finless Porpoise, *Neophcaena phocaena*	In-shore waters of Asia	[43]
Commerson's dolphin, *Cephalorhynchus commersonii*	Near-shore waters <100 m depth, including east coast of Argentina, southern Chile, & Indian Ocean	[40]
Hector's dolphin, *Cephalorhynchus hectori*	New Zealand coastal waters. Often in estuaries	[48]
Chilean/Black dolphin, *Cephalorhynchus eutropia*	Coastal Chile	[49]

Undoubtedly the major hindrance in answering whether these mammals do in fact exploit TWIPS is the lack of acoustic records which were taken in a manner specifically designed to determine the relevant features of the pulses. As stated above, the sampling frequency must be sufficiently great to allow robust analysis of the phase. Multi-element acquisition systems should be used to show undoubtedly that multi-pulses emanate from the species in question, and are not the result of environmental reflections as some investigators have proposed [43]. The environmental conditions must be sufficiently challenging to stimulate the cetacean to use twin-pulse techniques, if it is capable of that. The measurement must be at the spatial peak of the projected beam which *Cephalorynchus* and *Phocoena* produce, and not off-axis as is easily done given the narrow beamwidths observed [8, 11, 48, 50]. This is because TWIPS is dependent on nonlinear bubble dynamics, which in turn require high amplitude acoustic waves. Whilst careful measurements of the most closely studied dolphin (*Tursiops truncatus*, the Bottlenose dolphin, which is not a member of *Cephalorynchus* or *Phocoena* and does not produce twin pulses) has shown [41] that they can produce 126 kPa peak-to-peak at a range of 1 m, specific measurements of the type described above need to be undertaken to determine the maximum amplitudes which can be generated by *Cephalorynchus* and *Phocoena*. Whether or not cetaceans do indeed exploit TWIPS, the possibilities for man-made sonar applications have been demonstrated. The claim cannot be made that odontoceti use TWIPS: to quote Carl Sagan, "extraordinary claims require extraordinary evidence" and such evidence has not been obtained (the authors have not been able to obtain funding for such a study). However the object of the study was to determine whether the laws of physics would allow for the development a sonar which could operate in bubbly water, which Figure 23 proves, and as such the study says no more than would concur with Faraday when he said "Nothing is too wonderful

to be true if it be consistent with the laws of nature". That consistency has been demonstrated for TWIPS.

Investigators have been able to study biosonar detection capabilities in noisy [51] and surface reverberant environments [52, 53]. Interestingly, despite both the strategic importance of the acoustically-difficult littoral zone [54] and the well-known ability of certain odontoceti (especially those of the genus *Cephalorhynchus* [45-49]) to compete successfully in this habitat, there is little published work which reports on the acoustic abilities of dolphins in shallow-water conditions. Fertile ground for investigation could include observations and acoustic measurements of wild mammals which are indigenous to environments containing littoral zone challenges, such as the persistent presence of bubble clouds in their habitat. A suitable array could distinguish whether the multiple pulses are generated by individuals directly or through surface bounces (note that in principle TWIPS could work if the second pulse was generated by a surface bounced, provided it was sufficiently similar to the first pulse). It is of critical importance that the acoustic emissions of wild shallow-water species of odontoceti be non-invasively measured in conditions when microbubbles are present within the surf zone in sufficient numbers to confound standard sonar techniques (i.e. when weather, topography, wave conditions etc. are suitable). Such measurements should be made using multi-element arrays. While use of a sampling frequency about two times higher than the highest acoustic vocalisation is sufficient for basic investigations, it may not be sufficiently high to avoid signal distortion which would makes it difficult to perform detailed signal analysis.

Rigorous procedures for conducting measurements of odontoceti in captivity have a well-recognised history [41]. Hypothetically, it is possible to construct a thought-experiment whereby the range of observations of those mammals already in captivity could include ones to determine to what extent it is possible for them to detect, localise and identify fish and other solid objects in water (using well-recognised techniques [41]) containing a bubble populations resembling those found in the wild [2, 7, 17], and comparing this ability to that obtained with other populations (e.g. of large bubbles). Whilst acoustical techniques were used to measure the bubble populations in this paper, non-acoustic methods would be preferable if odontoceti are present [55]. Possible scenarios include one where the mammal is in bubble-free water and attempts to identify an object in the presence of a bubble screen; or where both the target and the mammal are in bubbly water. The experiment would be aimed at evaluating the performance of odontoceti in conditions containing elements which present difficulties to human sonar in shallow water (such as bubbles) and to determine the source of any enhanced performance (e.g. the characteristics of the platform, acoustics, processing etc.). Both active and, potentially, passive [56-58] techniques could considered. Measurements made in captivity are advantageous in that they make it possible to determine quantitatively the capability of an individual dolphin to find a given target in a particular condition. By varying any of these elements, it is possible to develop an overall picture of the ability of dolphins to locate targets despite a complex but controllable environment. Implementation of such a thought-experiment would be illegal to execute under UK law.

CAVITATION AND CETACEAN: THE ADVERSE EFFECTS OF ANTHROPOGENIC ACOUSTIC FIELDS

The impact of anthropogenic noise on marine mammals remains poorly understood. The most extreme examples of this impact are the mass strandings of cetaceans, temporally and spatially coincident with the use of mid-frequency military sonars. Initial stranding events [59] occurred before the causal link between sonar and strandings was hypothesised. Subsequent similar events are routinely the focus of investigations. In some cases these investigations have concluded that the sonars were directly implicated as causes of the strandings [60-62], whereas in other cases no evidence of a link to sonar has been determined (see, for example, reference [63]). For mass stranding events in which sonar is widely accepted as being a causal factor, the vast majority of animals affected are species of beaked whale. Consequently, considerable recent research effort has been dedicated to understanding the mechanisms which potentially lead to beaked whale strandings.

In several cases, necropsies performed on the stranded carcases reveal the presence of gas and fat emboli [61, 62] which are consistent with, but not diagnostic of, decompression sickness (DCS) [64]. Historically it has been assumed that marine mammal physiology prevents the

generation of bubbles which can lead to DCS [64, 65]. Whilst it is certainly true that evolutionary forces have mitigated the risks to marine mammals from DCS, it is overly simplistic to assume the absence of *in vivo* bubble generation. Indeed, there is increasing evidence of bubble formation in cetaceans in the absence of evidence of exposure to unusual anthropogenic noise [66, 67]. The pathology associated stranded animals exposed to sonar is distinct from the examples in references [66, 67] in that the embolisms are systemic rather localised. Further the examples in [66, 67] appear to have been the consequence of sustained non-lethal processes: for example in reference [67] some lesions are surrounded by fibrosis.

There are broadly two theories as to the mechanisms by which *in vivo* bubble formation occurs in beaked whales leading to DCS. The first is that the acoustic source directly leads to the growth/generation of bubbles [68], i.e., the acoustic field generated by the sonar source generates a population of relatively large bubbles. The second mechanism is that the sonar induces a behavioural response that causes DCS [69]. The diving behaviour of beaked whales has been poorly understood, but recent studies [69-71] have begun to provide data about typical dive profile for three species: Northern bottlenose whale (*Hyperoodon ampullatus*) [71], Cuvier's beaked whale (*Ziphius cavirostris*) [69, 70] and Blainville's beaked whale (*Mesoplodon densirostris*) [69, 70]. It seems highly likely that the typical diving behaviour of these animals is linked in some manner to their susceptibility to sonar. This may be either through a physical or a behavioural mechanism. It is almost certainly the case that both mechanisms have the potential to cause *in vivo* bubble generation. However, it is not apparent which will be the dominant mechanism under realistic conditions. For example one might consider two scenarios when a beaked whale encounters a sonar: first, the animal flees as a consequence of exposure to sonar, before a physical harm is incurred, but in doing such induces DSC; second, the animal incurs damage leading to DCS prior to, or in spite of, a behavioural response.

CONCLUSIONS

This paper has outlined a range of proposed methods by which cetaceans may be utilising the acoustical effects of gas bubbles to their advantage (such as in the generation of acoustical traps), or to mitigate the detrimental effects which bubbles have on active sonar. The ability of the authors to test these hypotheses have been limited by legislation and absence of funding. The experimental model scale bubble net only provided a very limited test, and lacks the refractive element, knowledge of the actually bubble population generated by the whales in the net, and a suitable scaled version of this for the experiment. TWIPS sonar has been used to detect targets in bubble clouds which are invisible to conventional sonar. The possibility that *odontocete* might use TWIPS is intriguing, but by no means settled: the question of whether the pulse amplitudes are sufficient, and whether the frequency range is appropriate, need to be settled. Furthermore there are those who adhere to the hypothesis that the second pulse is the result of a surface bounce, and not deliberately generated by the animal. It would be intriguing to investigate whether any of the species identified in Table 1 adapt their sonar for bubbly conditions, or show an enhanced ability in shallow water (their primary habitat) compared to free-ranging species, such as *Tursiops*, that have dominated testing and training by humans. There have been extensive recordings of the emissions of the Harbour Porpoise (*Phocoena phocoena*), a shallow-water animal. Harbour porpoise emissions have been analysed by our group for the presence of equi-amplitude phase-reversed pulse pairs, but no such acoustic emissions have yet been identified. However, regardless of these intriguing questions, man-made sonar has now been demonstrated as reaching the stage where TWIPS sonar can be experimentally demonstrated, which offers the possibilities not only for applications of sonar in shallow water, but also for a range of EM applications, including radar, lidar and THz radiation [35]. Finally, the possibility that anthropogenic noise and sonar could generate detrimental effects, including bubble activity, in cetaceans was addressed.

ACKNOWLEDGEMENTS

The material on humpback whale bubble nets and echolocation by odontoceti in bubbly water was unfunded. The authors are grateful to J. K. Dix for the loan of equipment and to him, G. Robb, D. Coles, G.T. Yim and C. Powles for volunteering of manual effort to assist with manoeuvring the sizeable items of equipment in the laboratory.
The authors acknowledge Paul Jepson for advice on the potential harmful effects of anthropogenic sonar.

References

References by TGL can be downloaded from
http://www.isvr.soton.ac.uk/STAFF/Pubs/pubs90.htm

[1] T. G. Leighton: From seas to surgeries, from babbling brooks to baby scans: The acoustics of gas bubbles in liquids', *International Journal of Modern Physics B,* **18** (2004) 3267-3314.
[2] T. G. Leighton, G. J. Heald: "Chapter 21: Very high frequency coastal acoustics," in Acoustical Oceanography: Sound in the Sea, H. Medwin, Ed. Cambridge University Press, (2005) pp. 518-547
[3] T. G. Leighton: What is ultrasound? *Progress in Biophysics and Molecular Biology*, **93** Issues 1-3 (2007) 3-83.
[4] T. G. Leighton: The Acoustic Bubble (Academic Press, London) (1994).
[5] T. G. Leighton: 'Nonlinear Bubble Dynamics And The Effects On Propagation Through Near-Surface Bubble Layers,' *High-Frequency Ocean Acoustics*, Eds. M.B. Porter, M. Siderius, and W. Kuperman, (American Institute of Physics Melville, New York) *AIP Conference Proceedings* **728** (2004) 180-193.
[6] T. G. Leighton, D. C. Finfer, P. R. White: Bubble acoustics: What can we learn from cetaceans about contrast enhancement? *Proc. 2005 IEEE International Ultrasonics Symposium* (Rotterdam) (2005) pp. 964-973.
[7] H. Medwin, Ed. Acoustical Oceanography: Sound in the Sea, Cambridge University Press (2005).
[8] T. G. Leighton, G. J. Heald, H. Griffiths, G. Griffiths (editors): *Acoustical Oceanography, Proceedings of the Institute of Acoustics* **23** Part 2 (2001).
[9] W. H., Munk, W. C. O'Reilly, J. L. Reid: Australia-Bermuda sound transmission experiment (1960) revisited. *J. Phys. Oceanogr.* **18** (1988) 1876-1898.
[10] S. Lee, M. Zanolin, A. M. Thode, R. T. Pappalardo, N. C. Makris: Probing Europa's interior with natural sound sources, *Icarus* **165** (2003) 144–167.
[11] T. G. Leighton, P. R. White: The sound of Titan: a role for acoustics in space exploration. *Acoustics Bulletin* **29** (2004) 16-23.
[12] T. G. Leighton, P. R. White, D. C. Finfer, E. J. Grover: The sounds of seas in space: the 'waterfalls' of Titan and the ice seas of Europa, *Proceedings of the Institute of Acoustics* (T. G. Leighton, editor) , **28**(1), (2006) 75-97.
[13] T. G. Leighton, P. R. White, D. C. Finfer: The sounds of seas in space, *Proc. Int. Conf. Underwater Acoustic Measurements, Technologies and Results* (J. Papadakis, L. Bjorno, editors) (2005) 833-840
[14] T. G. Leighton, The use of acoustics in space exploration, ISVR Technical Report (in press), May 2007.
[15] L. M. Brekhovskikh , Yu. P. Lysanov: Fundamentals of Ocean Acoustics (Springer Series on Wave Phenomenoa; Springer-Verlag), Second Edition (1991) Section 7.3.1.
[16] Seongil Kim, G. F. Edelmann, W. A. Kuperman, W. S. Hodgkiss, H. C. Song, T. Akal: Spatial resolution of time-reversal arrays in shallow water. J*ournal of the Acoustical Society of America* **110** (2001) 820-829.
[17] T. G. Leighton, S. D. Meers, P. R. White: Propagation through nonlinear time-dependent bubble clouds, and the estimation of bubble populations from measured acoustic characteristics, *Proceedings of the Royal Society A*, **460** (2004) 2521-2550.
[18] P. R. Birkin, T. G. Leighton, J. F. Power, M. D. Simpson, A. M. L. Vincotte, P. Joseph: Experimental and theoretical characterisation of sonochemical cells. Part 1. Cylindrical reactors and their use to calculate the speed of sound in aqueous solutions, *J. Phys. Chem. A*., **107** (2003) 306-320.
[19] T.G. Leighton, S.D. Richards, P.R. White: Trapped within a wall of sound: A possible mechanism for the bubble nets of humpback whales, *Acoustics Bulletin* **29** (2004) 24-29.
[20] F. A. Sharpe, L. M. Dill: The behaviour of Pacific herring schools in response to artificial humpback whale bubbles*, Canadian Journal of Zoology-Revue Canadienne de Zoologie* **75** (1997) 725-730.

[21] T. G. Leighton, D. C. Finfer, E. Grover, P. R. White: An acoustical hypothesis for the spiral bubble nets of humpback whales and the implications for whale feeding, *Acoustics Bulletin*, **22** (2007) 17-21.
[22] F. A. Sharpe: Social foraging of the southeast Alaskan Humpback whale, *Megaptera novaeangliae.* PhD Thesis, University of Washington (1984).
[23] F. E. Fish: Performance constraints on the manoeuvrability of flexible and rigid biological systems. *Proceedings of the Eleventh International Symposium on unmanned untethered Submersible Technology* (1999) 394-406.
[24] T. R. Kieckhefer: Humpback facts: a beginner's guide to a unique creature. *Upwellings* (publ. Pacific Ceatcean Group) (1996) pp. 4 -5.
[25] H. Williams, Whale Nation, Jonathan Cape (London) (1988).
[26] C. G. D'Vincent, R. M. Nilson, R. E. Hanna: Vocalization and coordinated feeding behaviour of the humpback whale in southeastern Alaska, *Sci. Rep. Whales Res. Inst.*, **36** (1985) 41-48.
[27] T. G. Leighton, S.D. Richards, P.R. White: Marine mammal signals in bubble water. *Proceedings of the Institute of Acoustics Symposium on Bio-sonar and Bioacoustics Systems, Proceedings of the Institute of Acoustics **26*** no. 6 (2004) 6 pages.
[28] T. G. Leighton, P. R. White, D. C. Finfer, S. D. Richards: Cetacean acoustics in bubbly water. *Proceedings of the International Conference on Underwater Acoustic Measurements, Technologies and Results*, (J. S. Papadakis and L. Bjorno, editors) (2005) pp. 891-898.
[29] W. Au, D. James, K. Andrews: High-frequency harmonics and source level of humpback whale songs, *J. Acoust. Soc. Am*., **110**, 2770 (2001).
[30] W. W. L. Au, Harbor porpoise (*Phocoena Phocoena*) acoustics: In memory of Anthony David Goodson. *Proceedings of the Institute of Acoustics Symposium on Bio-sonar and Bioacoustics Systems, Proceedings of the Institute of Acoustics* vol **26** no. 6 (2004).
[31] A. Byatt, A. Fothergill, M. Holmes and Sir D. Attenborough, *The Blue Planet*, BBC Consumer Publishing (2001).
[32] D. H. Simpson, Ting Chin Chien, P. N. Burns: 1999: Pulse inversion Doppler: a new method for detecting nonlinear echoes from microbubble contrast agents, *IEEE Transactions on Ultrasonics, Ferroelectrics and Frequency Control*, **46** (1999) 372-382.
[33] P. N. Burns, S. R. Wilson, D. H. Simpson: Pulse Inversion Imaging of Liver Blood Flow: Improved Method for Characterizing Focal Masses with Microbubble Contrast, *Invest. Radiol.* **35** (2000) 58-71.
[34] T. G. Leighton, P. R. White, D. C. Finfer: Bubble acoustics in shallow water: possible applications in Nature. *Proc. Int. Conf. on Boundary influences in high frequency, shallow water acoustics* (Bath) (2005) pp. 433-440.
[35] T. G. Leighton, P. R. White, D. C. Finfer: Target Detection in Bubbly Water. International patent application number PCT/GB2006/002335; claiming priority from UK patent application GB 0513031.5, University of Southampton, (2005).
[36] S. D. Meers, T.G. Leighton, J. W. L. Clarke, G. J. Heald, H. A. Dumbrell, P. R. White: The importance of bubble ring-up and pulse length in estimating the bubble distribution from propagation measurements," in *Acoustical Oceanography, Proceedings of the Institute of Acoustics,* (T. G. Leighton, G. J. Heald, H. Griffiths and G. Griffiths Eds., Bath University Press), vol. **23**(2), (2001) pp. 235-241.
[37] T. G. Leighton, D. C. Finfer, P. R. White: Sonar which penetrates bubble clouds, *Proceedings of the Second International Conference on Underwater Acoustic Measurements, Technologies and Results,* J.S. Papadakis and L. Bjorno, eds. (Crete) (2007) (in press).
[38] D. Coles, T. G. Leighton: Autonomous spar-buoy measurements of bubble populations under breaking waves in the Sea of the Hebrides (in press, this volume), 2007.
[39] O. Kreisher: Service Experts Eye 'Leap Ahead' In Mine Warfare Capabilities, *Seapower Magazine*, 2 pages (Sept. 2004).
[40] C. Kamminga, H. Wiersma H, Investigations on cetacean sonar II. Acoustical similarities and differences in *odontocete* sonar signals, *Aquatic Mammals*, **8**, pp. 41-62, 1981.
[41] W. W. L. Au: *The Sonar of Dolphins* (Springer-Verlag, New York), (1993).
[42] S. M. Dawson**,** C. W. Thorpe: A quantitative analysis of the sounds of Hector's dolphin. *Ethology* **86** (1990) 131-145.
[43] S. Li, K. Wang, D. Wang, T. Akamatsu: Echolocation signals of the free-ranging Yangtze finless porpoise (*Neophocaena phocaenoides asiaeorientialis*). *Journal of the Acoustical Society of America* **117** (2005) 3288-3296.

[44] H. Medwin: Specular scattering of underwater sound from a wind-driven surface, *Journal of the Acoustical Society of America*, **41** (1966) 1485-1495.
[45] F. B. Pichler, D. Robineau, R. N. P. Goodall, M. A. Meÿer, C. Olivarría, C. S. Baker: Origin and radiation of Southern Hemisphere coastal dolphins (genus *Cephalorhynchus*). *Molecular Ecology*, **10** (2001) 2215-2223.
[46] W. E. Evans, F. T. Awbrey, H. Hackbarth: High frequency pulses produced by free-ranging Commerson's dolphin (*Cephalorhynchus commersonii*) compared to those of Phocoenids. In: *Biology of the genus Cephalorhynchus*. Edited by R.L.B. Jr., G.P. Donovan. Cambridge: International Whale Commision, (1988) pp. 173-181.
[47] F. T. Awbrey, J. C. Norris, A. B. Hubbard, W. E. Evans: The bioacoustics of the Dall's porpoise salmon drift net interaction (San Diego), (1979).
[48] S. M. Dawson: The high-frequency sounds of Hector's dolphins *Cephalorhynchus hectori*. *Rep. Int. Whal. Commn. Spec. Issue*. **9** (1988) 339-344.
[49] R. N. P. Goodall, K. S. Norris, A. R. Galeazzi, J. A. Oporto, I. S. Cameron: On the Chilean dolphin, *Cephalorhynchus eutropia* (Gray, 1846). *Rep. Int. Whal. Commn. Spec. Issue*, (1988) pp. 197-257.
[50] B. Mohl, S. Andersen: Echolocation: high-frequency component in the click of the Harbour Porpoise (*Phocoena ph. L.*). *J. Acoust. Soc. Am.,* **54** (1973) 1368-1372.
[51] W. W. L. Au, R. H. Penner: Target Detection in Noise by Echolocating Atlantic Bottlenose Dolphins. *Journal of the Acoustical Society of America*, **70** (3) (1981):687-693
[52] W. W. L. Au, C. W. Turl: Target Detection in Reverberation by an Echolocating Atlantic Bottlenose Dolphin (Tursiops-Truncatus). *Journal of the Acoustical Society of America*, **73** (5) (1983):1676-1681.
[53] C. W. Turl, D. J. Skaar, W. W. Au: The Echolocation Ability of the Beluga (Delphinapterus-Leucas) to Detect Targets in Clutter. *Journal of the Acoustical Society of America*, **89** (2) (1991):896-901.
[54] S. Castelin, P. Bernstein: A notional scenario for the use of unmanned system groups in littoral warfare. In: *2004 IEEE/OES Autonomous Underwater Vehicles* (2004) 14-19.
[55] C. D. Serdula, M. R. Loewen: Experiments investigating the use of fiber-optic probes for measuring bubble-size distributions. *IEEE Journal of Oceanic Engineering*, **23** (4) (1998):385-399.
[56] P. Geißler, B. Jähne: Laboratory and inshore measurements of bubble size distributions, in *Natural physical processes associated with sea surface sound* (T. G. Leighton, editor, University of Southampton), (1997) 147-154.
[57] F. G. Wood, W. E. Evans: Adaptiveness and ecology of echolocation in toothed whales. In: Animal Sonar Systems. Edited by R.G. Busnel, J.F. Fish. New York: Plenum Press; 381-425, (1980)
[58] G. B. Deane, M. D. Stokes: Air Entrainment Processes and Bubble Size Distributions in the Surf Zone, *Journal of Physical Oceanography*, **29** (1999) 1393–1403.
[59] A. Frantzis: Does acoustic testing strand whales?, *Nature*, **392**, no. 6671 (1998) 29
[60] D. L. Evans, G.R. England (editors): Joint Interim Report Bahamas Marine Mammal Stranding Event of 14-16 March 2000, *US Department of Commerce (NOAA)/US Navy (*2001).
[61] A. Fernandez, J. F. Edwards, F. Rodriguez, A. E. de los Monteros, P. Herraez, P. Castro, J. R. Jaber, V. Martin, M. Arbelo: “Gas and fat embolic syndrome" involving a mass stranding of beaked whales (Family Ziphiidae) exposed to anthropogenic sonar signals, *Veterinary Pathology*, **42**, no. 4 (2005) 446-457.
[62] P. D. Jepson, M. Arbelo, R. Deaville, I. A. P. Patterson, P. Castro, J. R. Baker, E. Degollada, H. M. Ross, P. Herraez, A. M. Pocknell, F. Rodriguez, F. E. Howie, A. Espinosa, R. J. Reid, J. R. Jaber, V. Martin, A. A. Cunningham, A. Fernandez: Gas-bubble lesions in stranded cetaceans - Was sonar responsible for a spate of whale deaths after an Atlantic military exercise? *Nature*, **425**, no. 6958 (2003) 575-576.
[63] S. Norman, W. McLellan, D. A. Pabst, D. Ketten, S. Raverty, M. Fleetwood, J. K. Gaydos, S. Jefferies, T. M. Cox, B. Hanson, B. Norberg, L. Barre, D. Lambourn, S. Cramer: Preliminary Report: Multidisciplinary investigation of Harbour Porpoises (Phoncoena phoncoena) stranded in Washington states from 2 May - 2 June 2003 coinciding with the mid-range sonar exercise of the USS Shoup, 2004.
[64] S. H. Ridgway, R. Howard: Dolphins and the Bends, *Science*, **216**, no. 4546 (1982) 651.
[65] S. H. Ridgway, R. Howard: Dolphin lung collapse and intramuscular circulation during free diving - evidence from nitrogen washout, *Science*, **206**, no. 4423 (1979) 1182-1183.

[66] M. J. Moore, G. A. Early: Cumulative sperm whale bone damage and the bends, *Science*, **306**, no. 5705 (2004) 2215.
[67] P. D. Jepson, R. Deaville, I. A. P. Patterson, A. M. Pocknell, H. M. Ross, J. R. Baker, F. E. Howie, R. J. Reid, A. Colloff, A. A. Cunningham: Acute and chronic gas bubble lesions in cetaceans stranded in the United Kingdom, *Veterinary Pathology*, **42**, no. 3 (2005) 291-305.
[68] L. A. Crum, Y. Mao: Acoustically enhanced bubble growth at low frequencies and its implications for human diver and marine mammal safety, *Journal of the Acoustical Society of America*, **99** (1996) 2898-2907.
[69] P. L. Tyack, M. Johnson, N. A. Soto, A. Sturlese, P. T. Madsen: Extreme diving of beaked whales, *Journal of Experimental Biology*, **209**, no. 21 (2006) 4238-4253.
[70] R. W. Baird, D. L. Webster, D. J. McSweeney, A. D. Ligon, G. S. Schorr J. Barlow: Diving behaviour of Cuvier's (Ziphius cavirostris) and Blainville's (Mesoplodon densirostris) beaked whales in Hawaii," *Canadian Journal of Zoology-Revue Canadienne de Zoologie*, **84**, no. 8 (2006) 1120-1128.
[71] S. K. Hooker, R. W. Baird: Deep-diving behaviour of the northern bottlenose whale, Hyperoodon ampullatus (Cetacea : Ziphiidae), *Proceedings of the Royal Society of London Series B-Biological Sciences*, **266**, no. 1420 (1999) 671-676.